

UC Davis

UC Davis Electronic Theses and Dissertations

Title

MicroRNA-dependent regulation of caste and mating-status in the Honey Bee

Permalink

<https://escholarship.org/uc/item/6df7m28w>

Author

Jasper, William Cameron

Publication Date

2022

Supplemental Material

<https://escholarship.org/uc/item/6df7m28w#supplemental>

Peer reviewed|Thesis/dissertation

MicroRNA-dependent regulation of caste and mating-status in the Honey Bee

By

WILLIAM CAMERON JASPER
DISSERTATION

Submitted in partial satisfaction of the requirements for the degree of

DOCTOR OF PHILOSOPHY

in

Entomology

in the

OFFICE OF GRADUATE STUDIES

of the

UNIVERSITY OF CALIFORNIA

DAVIS

Approved:

Elina Niño, Chair

Joanna Chiu

Siobhan Brady

Committee in Charge

2022

Copyright © 2022 by William Cameron Jasper

Abstract

When an individual honey bee (*Apis mellifera*) changes in a hive, its' glandular output also changes. For example, a worker's mandibular glands (Mdg) typically produce larval food and other pheromones but in queen-less hives it will more closely resemble a queen's. As the biosynthesis of insect pheromones occurs in specialized tissues and involves regulatory modifications to conserved metabolic pathways, we hypothesized microRNAs (miRs), short (~22 nucleotide) RNA negative transcriptional modifiers and known regulators of metabolic pathways, would have significant roles in regulating pheromone production in honey bee Mdgs. We further hypothesized queen-less workers would have similar miR expression profiles as queens. Small RNA-Seq of the Mdg identified robust caste-specific (queen and worker) miRs profiles as well as a high number of previously undescribed miRs. Worker-expressed genes in the Mdg were enriched for predicted miR response elements (MREs) of miRs coherently up-regulated in both queens and queen-less workers with some ovary activation. In addition, novel worker-expressed genes were enriched for MREs of novel queen-expressed miRs. Predicted miR-protein-protein interaction networks identified potential regulatory hubs and detailed regulatory roles for individual miRs expressed according to caste and mating status. We also found putative worker pheromone biosynthesis genes expressed in queens are enriched for MREs of two worker-expressed miRs; ame-miR-31a-5p and ame-miR-92b-3p. Interestingly the two fatty acid synthase genes that may be expressed according to caste are predicted to contain the highest number of MREs for anti-correlated miRs of all putative

pheromone biosynthesis genes. MREs for ame-miR-375-3p that are highly up-regulated in queens and queen-less workers relative to queen-right workers, are enriched in genes down-regulated in queen-less workers relative to queen-right workers. Mandibular gland RNA-sequencing of queen-less worker bees fed an inhibitor for ame-miR-375-3p identified multiple genes involved in metabolic processes, autophagy, and stress responses reverting to the expression profile of a queen-right worker.

Introduction

Honey bees (*A. mellifera*) are eusocial animals and live in colonies comprised of a single reproductive female queen and typically tens of thousands of sterile workers who provide for the young, maintain and defend the hive, and forage for food [1]. Workers are well-studied examples of phenotypic plasticity where worker's phenotypic roles change in response to the larger needs of the hive [1]. A colony's ability to efficiently respond to the larger needs of the hive relies in large part upon a complex system of chemical communication where a worker's distinctive role is characterized by the output of its' many exocrine glands [1–3]. Queen's regulate worker behavior with a complex chemical signal produced by multiple glands that specifically inhibits swarming, the rearing of new queens, the onset of foraging behavior, dopamine expression in the worker brain, and juvenile hormone (JH) biosynthesis while promoting a retinue response and the expression of nurse-associated genes such as vitellogenin [4,5]. A worker retinue response consists of workers licking the queen and rubbing their antennae on her cuticle to then spread her signal throughout the colony. In the presence of a healthy queen signal, young workers feed worker-destined larvae with the secretions of two specialized glands, the hypopharyngeal and mandibular gland, comprised of proteins, fatty acids, and sugars [1,6]. Workers no longer receiving a queen signal will raise a new queen by moving a developing larvae into a specialized cell and provisioning it with an adjusted ratio of sugar,

proteinaceous and fatty acid secretions from the mandibular and hypopharyngeal glands commonly known as “royal jelly” [1,6].

The mandibular gland (Mdg) is a paired sac-like gland in the head attached to the mandible that primarily secretes fatty acid-derived pheromones in both workers and queens [7–13]. Worker Mdg are smaller than a queen’s and change output according to colony role [8,14–16]. Younger workers produce nursing-related free fatty acid compounds, 10-hydroxy-2-decenoic acid (10-HDA) being the primary compound [1,17–19]. 10-HDA has anti-inflammatory and histone deacetylase inhibition properties and is an important regulator of caste-specific larval developmental pathways [20,21]. As workers transition to foraging, the worker Mdg significantly increases production of 2-heptanone, once thought to be an alarm pheromone but may be a mild paralyzing agent [15,22]. As workers age, the Mdg displays structural differences as well as changes in the organelle composition in the various cell types within the ultrastructure, the most apparent being the composition of mitochondrial sub-types [15,17,23]. Specifically, during periods of high fatty acid production, the periphery of worker Mdg cells are populated with large mitochondria and large smooth endoplasmic reticulum [15,23].

Caste-specific blends of fatty acid-derived Mdg pheromones are product of a bifurcated biosynthesis pathway where genes related to fatty acid β -oxidation, amongst other cellular pathways, are expressed according to caste [4,8,14,24–26]. Glandular output in worker Mdgs as well as the underpinning gene expression is highly labile in conjunction with the shifting needs of the hive. For instance, Mdg

profiles of many workers in queen-less (QL) colonies will partially resemble that of a queen which then revert to “worker-like” upon introduction of a queen [4,8,14,27–29]. Foragers that return to brood-feeding duties are capable of re-activating brood-food biosynthesis pathways in their Mdgs [30,31]. While it has been demonstrated that the overall juvenile hormone (JH) levels and brain gene methylation profiles return to “nurse-like” state [30,32], much remains unknown regarding the molecular regulatory mechanisms underpinning phenotypic plasticity observed in Mdg.

Exocrine glands such as the Mdg are specialized animal secretory tissues where evolutionary, pleiotropic constraints typical of more conserved tissues are relaxed [33,34]. In such contexts, novel biosynthesis pathways emerge via the exaptation of deeply conserved metabolic gene modules [35–38]. A gene module can be defined as a cellular biochemical network, or patterns of connectedness between genes greater than those found in a randomly connected network [34]. The relaxed pleiotropic constraints that lead to the development of novel tissues are a significant source of evolutionary novelty where alterations to the regulatory regimen of gene modules are achieved, for instance, via sequence changes in transcription factor (TF) binding sites [34,35,39,40]. While transcriptional regulation is an important area of focus in understanding the origins of novel phenotypes, post-transcriptional regulatory actors, such as microRNAs, also deserve scrutiny [41–46].

MicroRNAs (miRs) are small (~22 nt) endogenous non-coding RNAs that regulate a myriad of biological processes by inhibiting the translation of specific target proteins [41,47]. In animals, the RNA-induced silencing complex (RiSC) binds

an miR with target messenger RNAs (mRNAs) via base pairing interactions to either degrade the mRNA or inhibit translation machinery [47]. MiR expression is often highly tissue specific and miR genomic diversity has been correlated to organismal complexity [44,45,47–49]. While a single miR binding site, or miR response element (MRE), often has a muted negative effect on protein level, miRs exert significant phenotypic effects upon single gene by having multiple and diverse MREs or via a single miR targeting multiple nodes within a cellular pathway [48,50–52]. Sequence divergences in MREs contribute to paralog neofunctionalization [53,54], a major evolutionary driver of specialization in novel tissues [55–57]. In such novel contexts, it is theorized that gene modules acquire novel regulatory apparatus via novel miRs more readily than TFs partially due to the deleterious pleiotropic effects novel TF binding domains may be more likely to confer [45,46,58–60]. Interestingly, the rise of novel miR families occur at a higher rates in animals relative to the rise of novel TF families [46]. Furthermore, novel miRs tend to emerge in scenarios of relaxed pleiotropic constraint such as specialized tissues or novel developmental contexts where it's predicted the more severe negative pleiotropic effects are avoided by novel miRs being relatively lowly expressed [46].

MiRs add robustness to cellular processes by stabilizing developmental switches, regulate biochemical bottlenecks and gene modules, acting as transcription buffers, and are fine-tuners of protein dosage [48,52,61]. The stabilization of gene expression by miRs canalizes phenotypes by augmenting the heritability of a trait and sharpening the action of natural selection [62]. Highly complex metabolic

networks are composed of smaller functional modules that sense a wide range of external input via sensory bottlenecks accordingly adjusting the expression of module enzymes [63]. The complex nature of metabolic networks allows for a greater potential of evolutionary exaptation where the functional modules can be duplicated and undergo neo-functionalization [36]. MiRs are well-known regulators of metabolic homeostasis as well as cross-talk between metabolic modules [52,64–66]. In particular, miRs have been shown to target network hubs and pathway bottle-necks of metabolic flows [52].

Insect pheromone biosynthesis pathways are derived from deeply conserved metabolic pathways and modules [37,38]. As metabolic pathways and modules are tightly regulated by microRNAs, we predict microRNAs will also have a significant role in the regulation of phenotypic plasticity observed in the honey bee Mdg. Furthermore, as queen-less worker Mdg gene expression and pheromone profiles resemble that of a queen, we predict the miR expression profile will as well. We also predict the inhibition of miRs coherently up-regulated in both queen-less workers and queens will act to return a queen-less Mdg transcriptional profile to a queen-right worker (“queen-right” meaning workers in a colony with a queen present). As exocrine tissues are theorized to be contexts of relaxed pleiotropic constraint, we further predict taxonomically restricted miRs will comprise a significant portion of expressed miRs while individually being lowly expressed. As worker-expressed genes are more likely to show signs of positive selection [67], we likewise predict enrichment

for MREs of taxonomically-restricted miRs amongst targeted genes to be more likely in workers than in queens.

Here, we use small RNA sequencing to quantify miR expression profiles of two honey bee tissues across multiple phenotypes and identify strong similarities in the in miR expression profiles of queens and queen-less workers relative to queen-right workers. We also identify many gene modules caste-expressed miRs are predicted to target. Additional RNA-sequencing of queen-less bee MGs where an miR showing high expression in both queen-less workers and queens relative to queen-right workers was inhibited showed many genes returning to a “queen-right”-like MG expression profile.

Results and discussion

MicroRNA expression clusters strongly according to caste and tissue type

In order to determine if miR expression correlated with caste and or mating status, we profiled small RNA expression of queens, queen-right workers, and queen-less workers with and without activated ovaries. We found miR expression in the mandibular gland correlated strongly with tissue type and caste (Fig 1, Table 1). Integrating the individual expression patterns of all differentially-expressed miRs using k-means clustering methods determined three miRNA expression clusters to be optimal. Sequencing data (Table S1) and pairwise comparisons (Table S2) across

multiple sample types are both provided in the supporting material.

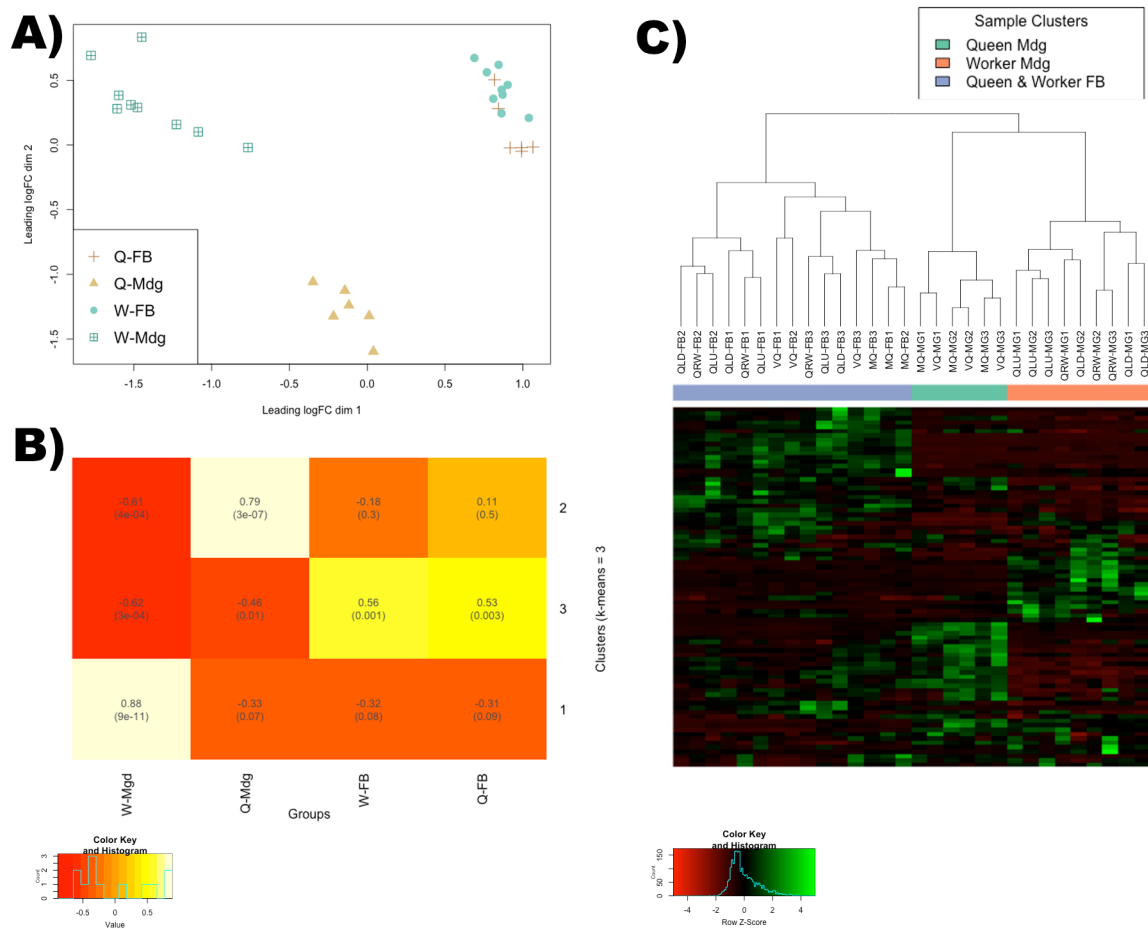


Fig. 1. MicroRNA expression clusters. A) Multidimensional scaling (MDS) plot of the miR expression of queen mandibular gland (“Q-Mdg” represented as gold triangles, n=6 samples: three virgin & three mated queens), worker mandibular gland (“W-Mdg” represented as aqua square grids, n=9 samples: three queen-right workers (QRW), three queen-less workers with un-developed ovaries (QLU), three queen-less workers with developed ovaries (QLD)), queen fat body (“Q-FB” represented as orange crosses, n=6 samples: three virgin & three mated queens), worker fat body (W-FB

represented as aqua circles. n=9 samples: three queen-right workers (QRW), three queen-less workers with un-developed ovaries (QLU), three queen-less workers with developed ovaries (QLD). B) Heat map of correlation between sample type and miR expression clusters as determined by k-means clustering. The values in the squares represent the correlation value to the group and the values in parentheses represent the calculated p value. Cluster 1 most strongly aligned with miR expression patterns of Q-Mdg samples, cluster 2 with W-Mdg samples, and cluster 3 with both Q-FB and W-FB samples). C) Hierarchical clustering of miR by co-expression modules. The expression of individual miR is displayed in a hierarchically clustered heatmap. Queen and worker fat body samples (blue) cluster together whereas queen (green) and worker (orange) Mdg show distinct co-expression patterns. Correlated miR expression intensity is shown in green where anti-correlated expression intensity is red.

Table 1. MicroRNA Co-expression Clusters

Cluster 1 (Mandibular Gland: Worker)	ame-miR-14-3p, ame-miR-278-3p, ame-miR-3049-5p, ame-miR-31a-5p, ame-miR-3759-3p, ame-miR-6043-3p, ame-miR-6047a-3p, ame-miR-6047a-5p, ame-miR-750-3p, ame-miR-92b-3p, ame-miR-932-5p, ame-miR-9883-5p, ame-miR-989-3p, ame-miR-993-3p, NC_037638.1_16823-3p, NC_037639.1_24322-3p, NC_037641.1_28636-3p
Cluster 2 (Mandibular Gland: Queen)	ame-bantam-3p, ame-let-7-5p, ame-miR-11-3p, ame-miR-12-5p, ame-miR-13a-3p, ame-miR-190-5p, ame-miR-275-3p, ame-miR-2765-5p, ame-miR-279a-3p, ame-miR-279b-3p, ame-miR-279c-3p, ame-miR-279d-3p, ame-miR-281-3p, ame-miR-283-5p, ame-miR-2944-3p, ame-miR-29b-3p, ame-miR-305-5p, ame-miR-306-5p, ame-miR-317-3p, ame-miR-34-5p, ame-miR-3477-5p, ame-miR-3718a-3p, ame-miR-3720-5p, ame-miR-375-3p, ame-miR-3785-3p, ame-miR-3791-3p, ame-miR-6005-5p, ame-miR-6037-3p, ame-miR-6040-3p, ame-miR-79-3p, ame-miR-8-3p, ame-miR-996-3p, NC_037648.1_3252-3P
Cluster 3 (Fat Body: Queen and Worker)	ame-miR-1-3p, ame-miR-10-5p, ame-miR-100-5p, ame-miR-125-5p, ame-miR-133-3p, ame-miR-137-3p, ame-miR-13b-3p, ame-miR-184-3p, ame-miR-193-3p, ame-miR-2-3p, ame-miR-252a-5p, ame-miR-252b-5p, ame-miR-263a-5p, ame-miR-263b-5p, ame-miR-276-3p, ame-miR-277-3p, ame-miR-2788-3p, ame-miR-2796-3p, ame-miR-282-5p, ame-miR-

	307-3p, ame-miR-315-5p, ame-miR-316-5p, ame-miR-3719-3p, ame-miR-3786-3p, ame-miR-3786-5p, ame-miR-7-5p, ame-miR-71-5p, ame-miR-87-3p, ame-miR-927a-5p, ame-miR-92a-3p, ame-miR-92c-3p, ame-miR-9a-5p
--	---

The table lists the individual honey bee microRNAs comprising microRNA expression clusters most strongly correlated with sample type as determined by k-means clustering.

Queen-less bees have “queen-like” miRNA expression patterns

Unsurprisingly, miRs differentially-expressed across tissues (DE-miRs) are comprised of miRs found within the above expression clusters (Table S2). Interestingly, in the mandibular gland, there is coherence in the relative direction of expression for many DE-miRs between queen-less and queen-right workers and between queens and queen-right workers (Table 2). There are 19 DE-miRs between Q-FB and W-FB and a single DE-miR between queen-less and queen-right workers (Table S3). Many fat body DE-miRs (11 of 19) are coherently expressed between queens and workers in the Mdg but the miRs often differ in the relative amount of total expression within each tissue. For instance, seven miRs, including ame-miR-375-3p and ame-miR-3477-5p, are up-regulated in queens relative to workers in both tissues but represent a larger percentage of the relative expression in the Mdg (Table S3, S4). There were no significant expression differences between mated queens and virgin queens. One possible factor in the lack of significant expression difference may have been that our mated queens were not observed to have laid any eggs. We were

unable to replicate queen egg-laying observed in our micro-hives that others reported [8].

Table 2. MicroRNA coherent expression

miR	miR Expression (LogFC)			MRE enrichment QL v QRW	
	Q v QRW	QLD v QRW	QLD v QLU	CDF	FE
ame-miR-11-3p	1.352	1.426	2.568	1.39E-05	1.26
ame-miR-3477-5p	1.287	1.178	1.379	1.85E-03	1.21
ame-miR-375-3p	1.135	1.125	0.767	2.08E-02	1.04
ame-miR-3785-3p		1.578	1.132		
ame-miR-7-5p	2.176		2.147	5.19E-11	1.24
ame-miR-14-3p	-1.387	-2.047	-2.429		
ame-miR-9883-5p	-3.751		-8.176		

Table 2 lists the miRs coherently regulated in queen mandibular glands and queen-less workers with developed ovaries workers versus queen-right workers and queen-less workers with un-developed ovaries. Numbers are the log fold change in expression of the first listed group versus the second. Also listed is the enrichment of miR response elements (MREs) within genes down-regulated in queen-less worker Mdgs relative to queen-right worker Mdgs (QL v QRW). Listed are significant cumulative distribution function (CDF) p values and the fold enrichment (FE) of the number of MREs within a set of genes relative to all genes.

Anti-Correlated expression of microRNAs and transcripts according to caste and mating status

To examine the regulatory roles of miRs in the contexts of caste and mating-status, we conducted a systems-level analysis integrating our miR expression and target prediction data with previously published mandibular gland RNA-Seq data [14]. As

miRs are known regulators of gene modules [52,64–66], we sought to elucidate specific modules important in caste and mating-status regulated by miRs up-regulated in the same context. To accomplish this, we generated multiple putative miR-Protein-Protein Interaction (mPPI) networks comprised of predicted miR-target pairings of up-regulated miRs and cognate predicted targets down-regulated in the same context (i.e. anti-correlated). Known protein-to-protein interactions between target genes with *Drosophila melanogaster* orthologs were taken from the BioGRID protein-to-protein interaction database [68]. First-degree interactor proteins were added and filtered by those with an *A.mel* ortholog predicted to be targeted by an anti-correlated miR (Table S7, S8). We then conducted network topological analysis on each network to identify potential regulatory interactions between up-regulated miRs and anti-correlated gene modules potentially relevant in glandular function.

Large mPPI networks comprised of the targets of all up-regulated miRs did not display significant degrees of network topology such as average number of neighbors, characteristic path length, clustering coefficient, or network density relative to random sets of genes (Table S5). This may be because of the large number of genes and 1st degree interactors comprising these mPPIs. Relatively smaller mPPIs comprised of the down-regulated targets of individual anti-correlated miRs displayed significant topology (Table S6) which comports with evidence that individual miRs regulate multiple nodes within a gene modules or biological pathways [48,50–52].

Predicted anti-correlated miR-target pairs with respect to caste

A vast majority (812/1028) of differentially-expressed genes (DEGs) down-regulated in Q-Mdg relative to W-Mdg [14] are predicted to be targeted by at least one anti-correlated miR (Table S7) underscoring a potentially significant role in caste phenotypes. [14] Each protein in the “QvW” mPPI is targeted by an average of 5.31 DE-miRs irrespective of the number of predicted MREs for a particular miR within a DEG (Table S8). The most highly targeted nodes are generally involved in structural or catalytic activities (Fig 2).

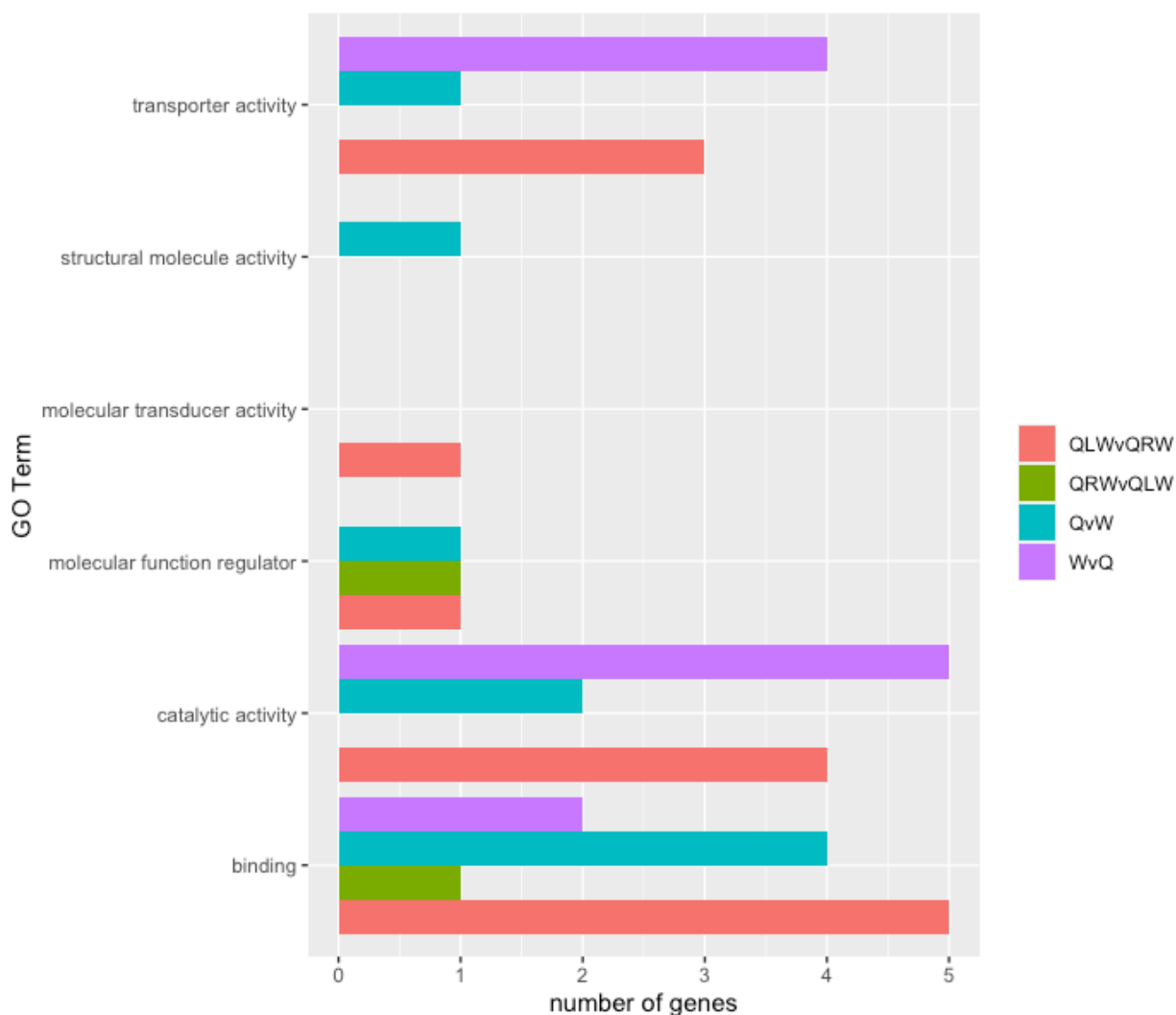


Fig. 2. Functional GO categories of highest predicted targeted DEGs. Number of genes in functional GO categories representing the top 20% predicted targets of anti-correlated miRs. “QvW” (white) is genes down-regulated in queens versus queen-right workers targeted by anti-correlated miRs. “WvQ” (pink) is genes down-regulated in queen-right workers versus queens. “QLWvQRW” (blue) is genes down-regulated in queen-less workers versus queen-right workers. “QRWvQLW” (green) is genes down-regulated in queen-right workers versus queen-less workers.

When considering the anti-correlated expression and predicted number of target genes, ame-miR-375-3p is putatively the most relevant miR (Fig 3A, 3B, Table S6). Ame-miR-375-3p accounts for a higher proportion of expression in Mdg samples relative to FB samples but is also expressed higher in queens in both tissues (Table S3). Interestingly, both ame-miR-3477-5p, and ame-miR-8-3p are predicted to target relatively few DEGs but represent a relatively high percentage of the overall miR expression profile in the mandibular gland relative to FB samples. Of note, Ame-miR-3477-5p is expressed higher in queens relative to workers in both tissues, while . Ame-miR-8-3p additionally represents a relatively high proportion of overall expression in the FB but does not display FB caste expression bias. Ame-miR-317-3p is expressed higher in queens in both tissues but displays no significant difference between tissues suggesting it may be a systemic regulator of caste. Ame-miR-34-5p is only expressed higher in Q-Mdg relative to QRW-Mdg and is slightly elevated, though statistically significantly, in W-FB relative to W-Mdg.

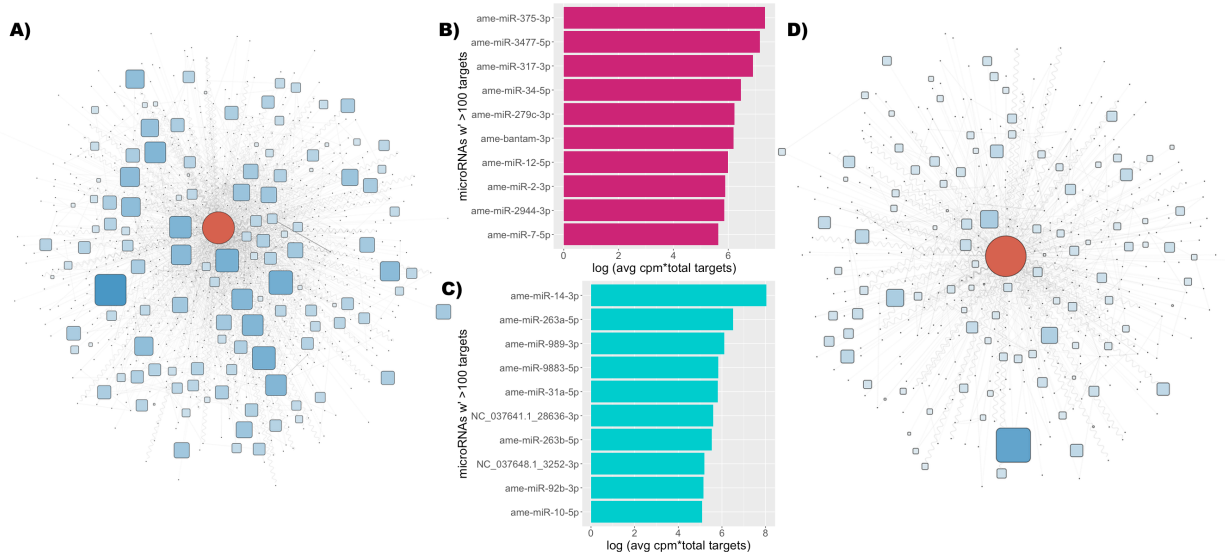


Fig. 3. Interaction networks of miRNAs with the highest expression changes and highest number of predicted targets. A) miR-protein-protein interaction (mPPI) network of ame-miR-375-3p, up-regulated in queens, predicted down-regulated protein targets in queens relative to queen-right workers (QRWs) with *Drosophila melanogaster* orthologs [14] and their first-degree interacting proteins with an *Apis mellifera* ortholog also predicted to be targeted by ame-miR-375-3p. Predicted down-regulated protein targets are shown in squares with rounded edges where the size and color intensity reflect up (red) or down (blue) regulation in terms of the log difference in average counts per million. First-degree interactors are not differentially-expressed and are shown as small points. Protein-protein and predicted miR-protein interactions are shown with straight lines where predicted miR-protein interactions with supporting evidence in *Drosophila melanogaster* are shown as wavy lines. B) Top ten log₂ values of the product of average counts per million for miRNAs up-regulated in queens relative to QRWs and total predicted targets among genes down-regulated in queens relative to QRWs [14]. C) Top ten log₂ values of the product of average

counts per million for miRs up-regulated in QRWs relative to queens and total predicted targets among genes down-regulated in QRWs relative to queens [14]. D) miR-protein-protein interaction (mPPI) network of ame-miR-14-3p, up-regulated in QRWs relative to queens, predicted down-regulated protein targets in QRWs relative to queens with *Drosophila melanogaster* orthologs [14], and their first-degree interacting proteins with an *Apis mellifera* ortholog also predicted to be targeted by ame-miR-14-3p.

The expression of miR-375-3p has been identified as an important regulator of pancreatic processes; a gland with both exocrine and endocrine functions related to the digestion and regulation of blood sugar levels [69–72]. MiR-375-3p is a putative biomarker for pancreatic cell death, diabetes, and prostate cancer and is known to regulate multiple aspects of pancreatic β -cell function, including clustering and islet formation, lipoapoptosis, phosphatidylinositol 3-kinase (PI3K) signaling, insulin exocytosis via Na⁺ channel regulation, glucose homeostasis, and vesicle fusion [64,69–80]. PI3K regulatory subunit alpha has multiple predicted MREs for ame-miR-375-3p and reverts to worker-like expression in antagomir-fed bees (Table S9). The U-Shaped (LOC100577801) transcription factor, a target of PI3K [81], regulates insect organ differentiation [82] has multiple predicted MREs for ame-miR-375-3p, but did not revert to a worker-like expression profile in antagomir-fed bees (Table S9) perhaps due to its' many predicted MREs for other caste-expressed miRs.

Mir-375-3p is heavily down-regulated in multiple types of cancer including gastric cancer cells where it targets a non-receptor tyrosine kinase and colorectal cancer cells where it targets MAP3K, a serine/threonine-specific protein kinase, jak2, a non-receptor tyrosine kinase, and Atg7, an autophagy pathway gene [83–85]. Tumor cells combat anoxic conditions by upregulating autophagy-related genes and miR-375-3p negatively regulates autophagy-associated genes in hepatocellular carcinoma cells [86]. In honey bees, ame-miR-375-3p is found in royal jelly, is expressed more highly in queen-destined larval development [87–91], is a potential regulator of juvenile hormone related genes [92], and involved in zygotic genome activation in early embryogenesis [89]. Knockdown of vitellogenin (*Vg*) in the worker fat body was found to decrease ame-miR-375-3p signal in the brain [93].

As with the “QvW” mPPI, most DEGs in the “WvQ” mPPI (1355/1601) are predicted to be targeted by at least one anti-correlated miR (Table S7). The 921 *D. melanogaster* orthologs of 1009 DEGs (Table S7, S8) account for approximately 63% of all down-regulated transcripts in this context [14]. Each protein in this mPPI network is targeted by an average of 5.1 DE-miRs (Table S8).

The DEGs with the most predicted targets primarily function in cellular transport and catalytic activity including regulation of organ growth and intracellular signal transduction (Fig 2). Ame-miR-14-3p is putatively the most influential miR in the context of QRW-Mdg given the degree of increase in expression relative to Q-Mdg that accounts for over 40% of total expression in QRW-Mdg (Fig 3C, 3D, Table S4) and is predicted to target ~16% of total targets (Table S6). While

still a large proportion of total expression in the Fb, ame-miR-14-3p represents a significantly larger proportion of expression in the Mdg (Table S3) and is not differentially-expressed according to caste in the Fb. Other putatively relevant miRs in this context include ame-miR-263a-5p, ame-miR-989-3p, ame-miR-9883-5p, ame-miR-31a-5p, and ame-miR-263b-5p. The majority of ame-miR-989-3p, ame-miR-31a-5p, and ame-miR-9883-5p, expression appears to be concentrated in the W-Mdg. Ame-miR-9883-5p is minimally expressed in all other assessed contexts. Ame-miR-989-3p and ame-miR-9883-5p only show significant up-regulation between W-Mdg and Q-Mdg and nowhere else assessed whereas ame-miR-31a-5p is up-regulated in Q-FB relative to both Q-Mdg and the W-FB in addition to up-regulation in W-Mdg relative to Q-Mdg. Roughly a third of anti-correlated genes are predicted to be targeted by ame-miR-9883-5p, a miR only known in honey bees, and ~37% are predicted to be targeted by ame-miR-989-3p. Ame-miR-263a-5p, already a high overall percentage of expression in Q-Mdg, is expressed more highly in W-Mdg by almost an order of magnitude representing the second most influence in terms of expression yet is predicted to target a relatively small proportion (approximately 10%) of anti-correlated genes. Furthermore, ame-miR-263a-5p is expressed more highly in the FB relative to the Mdg and more highly in the W-FB relative to Q-FB suggesting a role as a systematic regulator in the worker caste. Two novel miRs, NC_037641.1_28636-3p and NC_037648.1_3252-3p, are predicted to be relatively influential in the Mdg primarily based on the number of predicted target genes. While the expression of these two miRs is relatively low in the Mdg, of assessed tissues it is restricted to the

W-Mdg. Interestingly, the NC_037648.1_3252-3p is predicted to regulate the highest number of nodes (817) in this putative mPPI and ~50% of all down-regulated genes.

MiR-14-3p is involved in the regulation of fat metabolism, stress tolerance, as well aspects of calcium signaling associated with developmental apoptosis and autophagy in *D. melanogaster* [94–96]. MiR-14-3p levels are positively associated with stress tolerance and negatively associated with TAG and diacylglycerol (DAG) levels [96]. Lipid levels in insulin-producing neurosecretory cells in the brain, themselves theorized to have derived from hormone-producing pancreatic β cells, are regulated by the expression of miR-14-3p-target *sugarbabe* [97]. Inositol trisphosphate (IP3) and internal membrane-associated DAG are calcium signaling molecules that regulate autophagy flux and apoptosis [98,99]. An IP3 signaling pathway molecule, Inositol 1,4,5-trisphosphate kinase 2 (ip3k2), is directly targeted by miR-14-3p in *D. melanogaster* salivary glands where it regulates apoptosis and autophagy [94]. This effect was tissue-specific where systemic miR-14-3p loss or expression either prevented or precipitated, respectfully, stress-related apoptosis and autophagy in the salivary glands but not in the fat body [94]. Ame-miR-14-3p is also important in insect development [100,101] and one of the most highly expressed miRs in *Apis* royal jelly [91].

Predicted anti-correlated miR-target pairs with respect to reproductive status

As in previous comparisons, the majority (1531/2382) of genes down-regulated in queen-less bees mandibular glands (QL-Mdg) relative to QRW-Mdg [14] are predicted to be targeted by at least one anti-correlated miR (Table S7). The “QLWvQRW” mPPI

network, generated as previously described, contains 1101 *D. melanogaster* orthologs of 1207 DEGs accounting for approximately half of all down-regulated transcripts in this context (Table S7, S8). Proteins in this mPPI network are targeted by an average of 1.86 DE-miRs (Table S8). The anti-correlated DEGs predicted to be the most highly targeted are associated with multiple GO terms shown in Fig 2. As in the “QvW” mPPI, ame-miR-375-3p is predicted to influence gene expression most significantly given the degree of relative increase in expression, that it accounts for ~8% of total expression (Table S4), and the enrichment of MREs in anti-correlated genes (Table 2) where it is predicted to target 40% of anti-correlated genes (Table S6).

Slightly less than half (183/379) of the genes down-regulated in QRW-Mdg or QLU-Mdg relative to QLD-Mdg are predicted to be targeted by at least one anti-correlated miR (Table S7). The “QRvQL” mPPI network contains 134 *D. melanogaster* orthologs of 184 DEGs (Table S7, S8) and account for approximately half of all down-regulated transcripts in this context [14]. Proteins in this mPPI network are targeted by 1.48 DE-miRs (Table S8). As in “WvQ” mPPI, ame-miR-14-3p is putatively the most relevant miR in terms of association with a QRW-like state given its’ level down-regulation in QLD-Mdg relative to QRW-Mdg; a decrease from roughly half of total expression to about ten percent (Table S4).

Coherence of Anti-correlated Target MicroRNA-Gene Pairs in the Mandibular Gland between Queens and Queen-less Workers

To investigate the degree to which the “queen-like” mandibular gland phenotype is a property of gene regulation via microRNA, we quantified the coherence of anti-correlation, that is, predicted pairings of up-regulated miRs and cognate down-regulated predicted targets, shared between QLW-Mdg and Q-Mdg relative to QRW-Mdg. The threshold by which a gene was considered coherently down-regulated was simply if it was found to be significantly down-regulated in both cases [14].

In our Mdg dataset, more miRs were differentially-expressed in the Mdg with respect to caste (52) than mating status (11) (Table S3). In contrast, the number of genes seen expressed in the Mdg [14] were significantly differentially-expressed according to caste (2629) and mating status (2761) were roughly equivalent [14]. Seven caste-expressed miRs show coherency in expression direction (Table 2). Interestingly, only a small percentage (~12%) of DEGs down-regulated in QLW-Mdg relative to QRW-Mdg are also down-regulated in Q-Mdg relative to QRW-Mdg (Table S10). Of the 243 total DEGs coherently expressed between queens and queen-less workers, 151 are predicted to be targeted by coherently up-regulated miRs (Table S11). The most significantly enriched GO categories of coherently targeted genes were either related to regulation of developmental, structural, or metabolic processes (Fig S1).

Anti-correlated target-miR pairs coherent between Q-Mdg and QLW-Mdg of note include many transcription factors and other effectors of transcription (Table S11). The transcription factor Ken, predicted to be targeted by both ame-miR-375-3p and ame-miR-7-5p, is an established negative regulator of select components of the

JAK/STAT pathway in *D.mel* which transmits extracellular signals to the nucleus [102]. Ken is intermittently expressed during *D. melanogaster* development across multiple tissues [102]. Regulation of JAK/STAT components according to caste in the Mdg would align with the suggestion that developmental plasticity is achieved via selective regulation of this pathway [102]. Activating transcription factor 3 (ATF3), a negative regulator of the toll-like receptor pathways [103], is involved in a wide array of cellular stress responses [104–106], most interestingly so in pancreatic β -cells where it is up-regulated in the context of high concentrations of palmitate [107]. T-box genes are a diverse group of metazoan limb and organ developmental regulators [108]. The groucho protein, predicted to be targeted by ame-miR-11-3p and ame-miR-7-5p, is a member of a protein family of transcriptional co-repressors required for multiple developmental pathways including Notch and Wnt [109]. Dead ringer (dri) is a transcription factor essential in the development of the nervous system, salivary gland ducts, and cell shape in *D.mel* and is also expressed in salivary gland ducts [110–112].

The relatively low number of coherently expressed genes between queens and queen-less workers may highlight potential function in active reproduction in honey bees irrespective of caste. Interestingly, MREs for four of the five coherently up-regulated miRs in queens and queen-less workers (Table 2) are significantly enriched in genes down-regulated in queen-less workers relative to queen-right workers but not in genes down-regulated in queens. Investigations into the relatively larger

proportion of non-caste-expressed genes regulated by mating status-associated miRs may provide mechanistic insight into worker-specific reproduction.

Taxonomically restricted miRs target genes expressed according to caste

Taxonomically-restricted genes represent the majority of overall expression in specialized glands such as the Mdg and are important in the evolution of eusociality [67,113,114]. In the honey bee brain, taxonomically restricted miRs are more likely to target novel genes [115] supporting the idea that genes and cognate regulatory apparatus evolve in parallel. In the Mdg, novel miRs represent an overall large population of expressed miRs (107/188) but represent a small proportion (~1%) of overall expression (Table S4) consistent with predictions that novel miRs are weakly expressed, fast evolving, and expressed in a tissue-specific manner [46]. Biased expression of novel miRs in novel tissues theoretically minimizes larger deleterious fitness effects and underscores the likely role of novel miRs in the evolution of novel tissue [58,60]. While a bias in novel miRs targeting novel genes was observed in the brain, a relatively “conserved” tissue, neither genes with a bias in caste-specific expression nor signatures of positive selection were enriched for novel MREs [115]. In honey bees, neither the overall taxonomic restriction of expressed miRs, nor the taxonomic restriction of anti-correlated target genes with a bias in caste-specific expression has been investigated in a specialized tissue where novel and genes with caste-specific expression biases are primarily expressed.

For this analysis, we considered any miR or gene found only in Hymenopteran species as “novel” according to miRbase (miRbase.org) or MirGeneDB (mirgenedb.org). In the transcriptional networks of derived honey bee tissues, novel genes tend to have fewer interactions with other genes and are more likely to be expressed in bulk [113]. As previously observed [113], novel genes make up a larger portion of overall expression in the mandibular gland relative to the percent of genes expressed (Table S12). While this is true for both worker and queen genes, the pattern is much more extreme in genes upregulated in queen (Table S12). The higher relative expression of novel genes in the queen mandibular gland may be, in part, due to its’ large size relative to workers and that novel genes in honey bee social glands tend to be highly expressed genes related to the biosynthesis of glandular products [113]. Interestingly, this pattern also remains in genes up-regulated in queen-less workers relative to queen-right workers (Table S12) suggesting that, despite it being relatively smaller, mimicking queen-like pheromone profiles requires a higher proportion of novel gene expression. However, very few genes up-regulated in queen-less workers relative to queen-right workers are expressed coherently in queens relative to queen-right workers [14].

Among genes expressed according to caste in the Mdg, we tested for enrichment with respect to taxonomic restriction of both DE-miR and their predicted anti-correlated targets. Worker-expressed genes, irrespective of taxonomic restriction status, were enriched for MREs of novel DE-miRs and de-enriched for conservative DE-miRs (Table 3, S13). Further, worker-expressed novel genes were also enriched

for MREs of novel DE-miRs (Table S13). Perhaps in contrast, all queen-expressed genes were enriched for MREs of conserved miRs up-regulated in workers (Table 3, S13). As previously noted (Table 2), all worker-expressed genes, irrespective of taxonomic restriction, down-regulated in queen-less workers are highly enriched for anti-correlated miRs primarily composed of miRs coherently up-regulated in queens and queen-less workers. However, in contrast to genes down-regulated in queens, genes down-regulated in queen-less workers are enriched for conserved miRs.

Table 3. MRE enrichment by taxonomic restriction

	QvW:	CDF	FC	WvQ:	CDF	FC	QLWvQRW:	CDF	FC
Conserved DE-miR MRE in:									
Conserved DEG				enriched	3.92E-08	1.11	enriched	4.8E-05	1.09
Novel DEG				enriched	1.3E-06	1.10	enriched	6.1E-09	1.14
all DEGs				enriched	9.08E-13	1.10	enriched	6E-12	1.12
Novel DE-miR MRE in:									
Conserved DEG									
Novel DEG	enriched	0.004	1.13						
all DEGs	enriched	0.03	1.06						
Total DE-miR MREs in:									
Conserved DEGs							enriched	2.73E-05	1.09
Novel DEGs							enriched	1.24E-07	1.1
All DEGs							enriched	4.03E-11	1.1

Table 3 lists target enrichment of class of DE-miRs (conserved or novel) by class of gene (conserved or novel). “Novel” is short-hand for miRs or genes known only in the order Hymenoptera. We also tested for enrichment within gene class irrespective of DE-miR class. Calculated cumulative distribution function “CDF” values under 0.05 and a fold change above 1 were considered “enriched” (below 1 “de-enriched”). “QvW” is up-regulated miRs and down-regulated predicted (anti-correlated) gene targets in queens versus queen-right workers. “WvQ” is up-regulated miRs and anti-correlated

gene targets in queen-right workers versus queens. “QLWvQRW” is up-regulated miRs and anti-correlated gene targets in queen-less workers versus queen-right workers.

Table 4. Individual DE-miR MRE enrichment in anti-correlated DEGs by class

miR	enriched targets in	miR class	Conserved DEGs		Novel DEGs		All DEGs	
			CDF	FE	CDF	FE	CDF	FE
ame-miR-3785-3p	QvW	novel			9.864E-03	1.41		
ame-miR-3786-3p	QvW	novel			4.999E-02	1.09		
ame-miR-6040-3p	QvW	novel			3.599E-02	1.28		
ame-miR-263a-5p	WvQ	conserved	1.864E-05	1.57	1.273E-04	1.56	1.41E-08	1.56
ame-miR-263b-5p	WvQ	conserved			6.696E-04	1.30	9.23E-03	1.15
ame-miR-3049-5p	WvQ	conserved					3.53E-02	1.06
ame-miR-31a-5p	WvQ	conserved	3.613E-06	1.31	3.471E-02	1.13	3.78E-06	1.22
ame-miR-92a-3p	WvQ	conserved			2.805E-02	1.13	4.19E-02	1.08
ame-miR-92b-3p	WvQ	conserved	4.286E-03	1.27	3.200E-02	1.18	7.06E-04	1.23
ame-miR-989-3p	WvQ	conserved	4.357E-03	1.13	1.655E-03	1.15	4.45E-05	1.14
ame-miR-993-3p	WvQ	conserved	2.045E-04	1.33			8.28E-03	1.15
NC_037638.1_16823-3p	WvQ	novel	3.031E-02	1.15				
ame-miR-6047a-5p	WvQ	novel	5.423E-03	1.13	2.629E-04	1.19	1.66E-05	1.16
ame-miR-750-3p	WvQ	conserved					1.92E-02	1.18
ame-miR-11-3p	QLWvQRW	conserved	2.293E-04	1.30	9.428E-03	1.21	1.39E-05	1.26
ame-miR-3477-5p	QLWvQRW	conserved	1.957E-03	1.29			1.85E-03	1.21
ame-miR-375-3p	QLWvQRW	conserved			1.297E-03	1.09	2.08E-02	1.04
ame-miR-7-5p	QLWvQRW	conserved	5.454E-06	1.23	1.197E-06	1.24	5.19E-11	1.24

Table 4 [48] lists individual DE-miR enrichment by class within anti-correlated DEGs by class.

Novel miRs are expressed in both queens and workers but display distinct differences in terms of their enrichment within anti-correlated targets. The novel DEGs down-regulated in queens are significantly enriched for MREs of anti-correlated novel miRs while the novel miRs up-regulated in workers, while having a relatively high raw number of MREs, are not significantly enriched within anti-correlated targets, which may suggest worker novel miRs regulate these targets in

multiple contexts. Two of the eight worker-expressed novel miRs, ame-miR-6047a-5p and NC_037638.1_16823-3p, have MREs enriched in novel anti-correlated targets (Table 4, S13). Worker-biased genes are enriched for MREs of three of the five novel queen-expressed miRs; ame-miR-3785-3p, ame-miR-3786-3p, and ame-miR-6040-3p (Table 4, S13).

In the brain, worker-expressed genes are enriched for signatures of positive selection [67] but not for MREs of novel miRs [115]. Additionally, genes with signatures of positive selection in honey bees tend to generally be involved in processes associated with caste such as cell signaling, oxidative phosphorylation, and related processes [67,116]. Our findings in a derived “social” gland somewhat contrast a previous study [115] where we find novel worker-expressed genes are enriched for MREs of novel queen-expressed miRs (Table 3, 4). That is, maintaining the queen phenotype in the MG involves the down-regulation of worker genes enriched for MREs of queen-expressed novel miRs (Table 3, 4, S13). In contrast we see the queen-right worker MG phenotype comprises the down-regulation of queen-expressed genes and enrichment for conservative queen-expressed miRs. The queen-less worker phenotype comprises the down-regulation of some genes also down-regulated in queens but primarily consists of other queen-right worker-expressed genes not differentially-expressed between queens and queen-right workers. Interestingly however, all genes down-regulated in queen-less workers relative to queen-right workers are enriched for miRs, mostly conserved, coherently expressed in both queens and queen-less workers (Table 3, S13). In other words, a sub-set of queen-

expressed miRs may be significantly impactful in the queen-less phenotype. Only one novel worker up-regulated miR (NC_037638.1_16823-3p) showed any enrichment in queen-expressed genes and only in conserved genes (Table S13). Our results suggest that when evaluating the role of novel miRs in the evolution of eusociality or any novel function, it is important to consider both the degree of specialization with respect to tissue, the context of target expression, the biological pathways involved, and the enrichment of MREs of context-expressed miRs. Although the degree of positive selection was not evaluated amongst caste-specific genes in the Mdg, assuming that worker genes, in general, show higher signs of positive selection relative to queens, our results may suggest that the emergence of novel miRs may be more relevant in the context of maintaining the queen phenotype where the expression of more recently evolved worker genes may be deleterious. It is also interesting that novel queen-expressed genes in the worker Mdg are more enriched for MREs of conservative worker-expressed miRs and it would be interesting to determine the extent to which these patterns are true in other social glands. As such, the role of novel miRs in the evolution of eusociality, and, more broadly, the role of novel miRs in the emergence of novel tissues, should be further explored in a larger study examining the targets of expressed miRs in multiple tissue types by social context.

Predicted MREs of Putative Pheromone Biosynthesis Genes

Previous studies have identified putative pheromone biosynthesis genes (PPBGs) expressed according to caste [8,14] potentially involved in the biosynthesis of caste-specific blends of fatty acid-derived pheromones (Table S14). In order to examine the predicted regulatory roles of miRs expressed according to caste upon PPBGs, we filtered predicted MREs of anti-correlated DE-miRs within PPBGs and tested for statistical enrichment (Table S13, S14). We found that ame-miR-31a-5p, that is up-regulated in Q-FB vs W-FB, and ame-miR-92b-3p were enriched within PPBGs down-regulated in workers (Table S13).

Gene duplication can generate novel functionality partially via diversification of regulatory regimes, such as MRE divergences in paralogs [53,54]. Honey bees have two putative fatty acid synthase (FAS) paralogs (LOC411959 and LOC412815) which some evidence suggests may be expressed according to caste in the Mdg. In a microarray study, LOC411959 was up-regulated in queens and LOC412815 up-regulated in workers [8]. However, this result was not replicated in a subsequent RNA-Seq study, although LOC412815 was down-regulated in QLW-Mdg relative to QRW-Mdg [14]. Interestingly, the two FAS genes are predicted to be the two most targeted PPBGs by cognate anti-correlated miRs (Table S14). Multiple miRs have been identified as regulators of FAS and its' dysregulation in cancer [117–129]. Both FAS paralogs share predicted MREs for 88 miRs whereas 170 predicted MREs are unique to LOC411959 and 69 unique to LOC412815 (data not shown). The high number and diversity of predicted FAS MREs suggests FAS paralogs may be divergently regulated in multiple tissue contexts.

Cytochrome P450 monooxygenases are a diverse class of metabolic enzymes integral to many biological processes including toxin catabolism and the biosynthesis of chemical signals [8,14,24,130–132]. Multiple P450 genes with biases in expression by caste are amongst the genes with the highest number of predicted targets (Table S14). Caste-specific expression of P450s, suggests derived roles in modifications of fatty acid pheromone precursors such as the caste-specific hydroxylation of steric acid [8,14,24]. Cyp4G11, 6AS5, and 6A1, coherently expressed and regulated by multiple miRs up-regulated in both Q-Mdg and Q_{LW}-Mdg have been shown to be expressed in multiple tissues and are speculated to have roles in detoxifying xenobiotics [14]. An ortholog of Cyp4G11 in *D.mel* acts as an oxidative carbonylase upon aldehyde reduction from very long-chain acyl-CoA thioesters, via acyl-CoA reductases [133]. A probable cytochrome P450 6a14 is heavily down-regulated in queen Mdgs relative to workers [14] where RNAi knockouts in workers significantly reduce 10-HDA production [24]. Interestingly, 6a14 contains predicted MREs for anti-correlated miRs ame-miR-34-5p, ame-miR-3786-5p as well as ame-miR-6040-3p, the most significantly queen up-regulated miR.

A putative homolog of aldehyde dehydrogenase family 7 member A1 (LOC411140) is predicted to catalyze the conversion of 9-HDA to 9-ODA [8,14] contains MREs for six miRs showing significant anti-correlated expression (Table S14).

Other miRs that target many PPBGs include ame-miR-34-5p that has been previously identified as a 20-hydroxyecdysone-responsive critical developmental

regulator in insects [134], specifically of insect segmentation where, in honey bees, it targets multiple pair-rule and cytoskeletal genes [134,135]. Its' expression is also associated with glucose and lipid metabolism regulation in mice [136] as well as stress-response [137–139]. As previously mentioned, ame-miR-9883-5p is taxonomically restricted to *A.mel*. MiR-989-3p, an miR present so far only in the Endopterygota, has a bias in expression in female ovaries where it is required for ovary development [140–143] and has also been shown to target the sex-determining gene *doublesex* in *Bactrocera dorsalis* [141].

Inhibition of ame-miR-375-3p Alters Expression of Genes Expressed by Caste

We predicted that the miRs most likely to influence a “Q-Mdg-like” transcriptional profile in workers would be up-regulated in both QLW-Mdg and in Q-Mdg relative to QRW-Mdg and that inhibition of these miRs would have the greatest potential to return QLW-Mdg to a “QRW-like” transcriptional state. In an attempt to test our hypothesis, we targeted ame-miR-375-3p and ame-miR-7-5p for inhibition based on a criteria of high expression in QLW-Mdg as well as high number of predicted MREs amongst genes with caste-specific biases in both queens and in queen-less worker Mdgs (Table S6). Ame-miR-375-3p was predicted to have an optimal combination of high expression in Q-Mdg and QLW-Mdg relative to QRW-Mdg with a high number of predicted MREs amongst anti-correlated genes. We also chose ame-miR-7-5p given the relatively high number of predicted contextual targets.

Approximately one thousand genes were differentially-expressed between queen-less bees fed the antagomir antisense to ame-miR-375-3p and bees fed sugar only (Table S9). No DEGs were found between bees fed the ame-miR-7-5p antagomir and controls and a single gene, probable cyclin-dependent serine/threonine-protein kinase DDB_G0292550, was differentially-expressed between bees fed the scrambled control and bees fed sugar. A majority of DEGs (746) were expressed more highly in bees fed the inhibitor than control bees and include genes relevant with respect to caste, mating status, or pheromone biosynthesis [8,14,17]. Many up-regulated DEGs mimic “worker-like” profiles relative to queens and queen-less workers (Fig 4A, 4C, 4D).

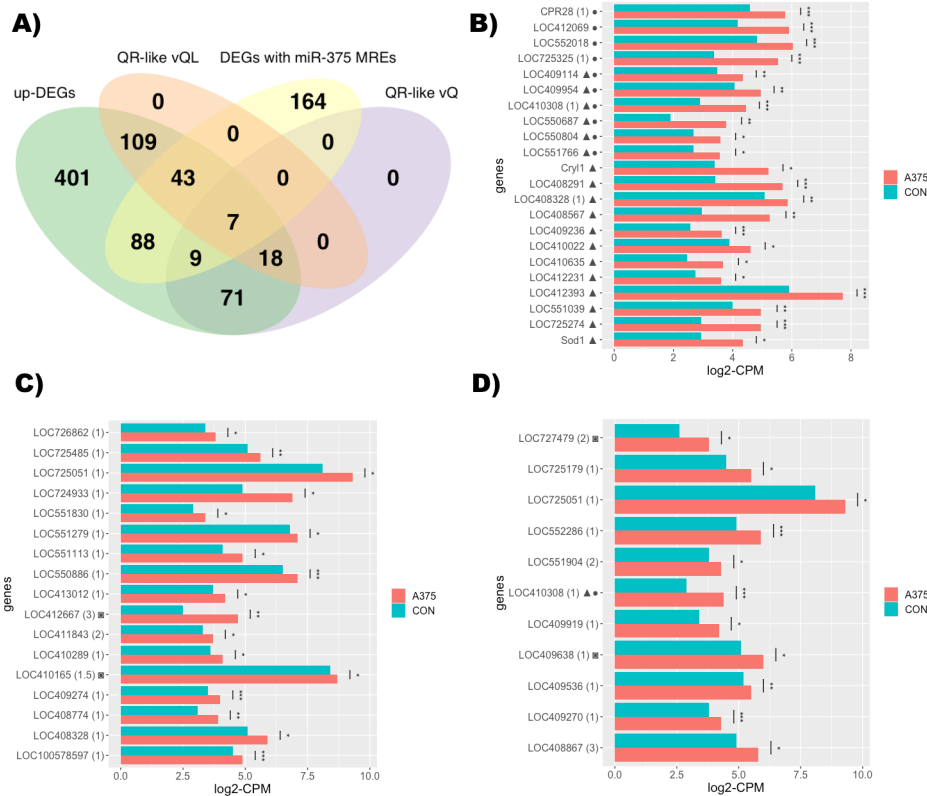


Fig. 4. Up-regulated genes in antagomir-fed queen-less bees. A) Venn diagram of total up-regulated genes in antagomir-fed queen-less bees relative to queen-less control bees (“up-DEGs” green), those also expressed higher in QRW-Mdg relative QLW-Mdg (“QR-like vs. QL”, orange), those up-regulated in W-Mdg relative to Q-Mdg (“QR-like vs. Q”, purple) and those with MREs for ame-miR-375-3p (“DEGs with miR-375 MREs”, yellow). B) DEGs increasing in expression in antagomir-fed bees also seen highly expressed in worker bees with higher 10-HDA production (circle symbols, [17]) as well as mitochondrial genes in worker-destined larvae (triangle symbols, [144]). Adjusted p-values are shown with asterisks (adj.P.Val < 0.05 “*”, < 0.01 “**”, and < 0.005 “***”). Expression of genes in bees fed antagomir for ame-miR-375-3p (“A375”) are shown in red and control queen-less bees (“CON”) are shown in blue. The number of predicted MREs for ame-miR-375-3p within the gene are shown in parenthesis. C) DEGs returning to a “worker-like” expression pattern involved in autophagy, traffic, secretion, and cell signaling. DEGs with square symbols are expressed lower coherently in both queens and queen-less workers relative to queen-right workers D) DEGs returning to a “worker-like” expression pattern involved in fatty acid metabolism or pheromone production.

Many DEGs are also predicted to be targeted by ame-miR-375-3p and, of those, many are up-regulated relative to controls suggesting at least a partial inhibitory effect of the antagomir localized in the mandibular gland (Fig 4A). While the direction of expression of ame-miR-375-3p is coherent in the FB and Mdgs between workers

and queens, the magnitude of expression difference observed between QRW and QLW in the Mdg is not observed in the Fb (Table S3, S4). While we cannot exclude all changes in expression are a result of a systemic effect of the antagomir, ame-miR-375-3p is expressed in higher proportion in the Mdg relative to the Fb, as well as the differential expression observed amongst queen-less and queen-right groups, suggesting a local effect of the antagomir in the mandibular gland is reasonable. Furthermore, as tissue-specific miR expression is correlated with miRs binding to MREs with lower binding affinities [145], it may be that inhibition of an miR highly expressed in a particular tissue may affect the expression of genes containing MREs that did not meet prediction thresholds.

The vast majority (>80%) of up-regulated *D. melanogaster* orthologs in the generated PPI sub-network are significantly associated with GO terms related to energy and metabolic processes (Fig 5). Network analysis of the PPI showed significance with respect to the average number of neighbors and clustering coefficient of up-regulated genes relative to all genes (Table S15).

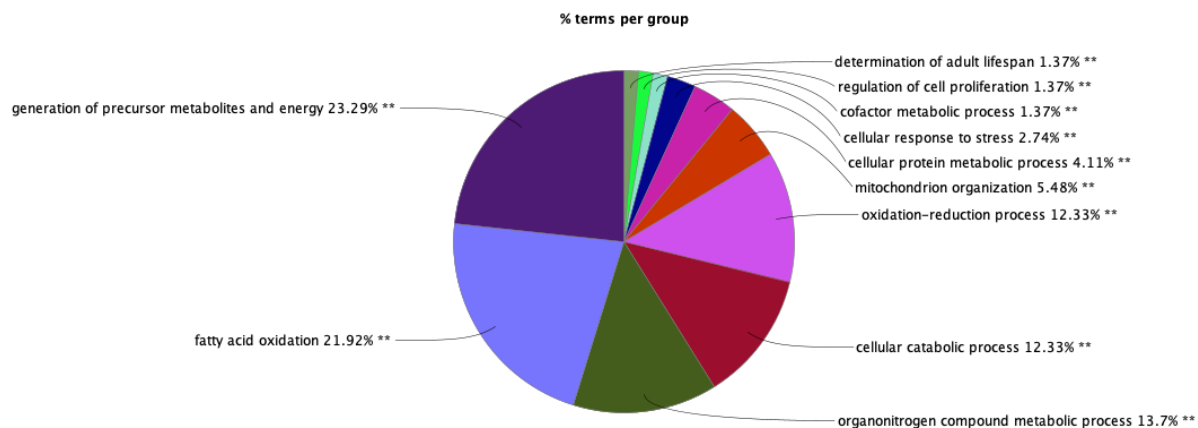


Fig. 5. GO terms associated with up-regulated genes in bees fed antagomir for ame-miR-375-3p. GO terms generated via ClueGO analysis of upregulated genes.

Predicted Regulation of Gene Pathways by Coherently-Upregulated MicroRNAs

Many genes and proteins expressed in the worker Mdg with respect to the presence of a queen are putatively involved in insect pheromone biosynthesis [8,14,24]. Interestingly, genes, some with predicted MREs for ame-miR-375-3p, associated with 10-HDA production in the worker mandibular gland [17] as well as genes differentially-expressed between queen and worker larvae [144] return to a “worker-like” expression profile in antagomir-fed bees (Fig 4B). Worker production of 10-hydroxydecanoic acid (10-HDA) is associated with higher counts of proteins associated with fatty acid metabolism, carbohydrate metabolism, pheromone biosynthesis, as well as protein metabolism, protein folding, cell signaling, major royal jelly proteins, detoxification, developmental, and structural pathways [17]. As ame-miR-375-3p is expressed higher in QLW-Mdg and Q-Mdg relative to QRW-Mdg, and, theoretically, is functional in the “queen-like” transcriptional state of the worker, we will discuss genes that return to a “QRW-like” expression profile upon inhibition of ame-miR-375-3p in QLWs in the supplemental discussion. There, we first focus on genes biased in expression towards QRW-Mdg and the production of worker pheromones, have a predicted MRE for ame-miR-375-3p, and that are higher in expression in queen-less bees fed ame-miR-375-3p inhibitor relative to queen-less

control bees. Upon inhibition of *ame-miR-375-3p* in queen-less workers, we observed genes involved in autophagy, cell trafficking, and secretion (Fig 4C) as well as pheromone production and fatty acid and energy metabolism genes (Fig 4D) increasing in expression to more resemble expression states observed in queen-right worker among other categories of genes. All genes discussed in the supplemental section fit this expression profile and have at least one predicted MRE for *ame-miR-375-3p* unless noted. In each section, we will also discuss other relevant genes predicted to be targeted by *ame-miR-375-3p* but not differentially-expressed in our TAG-Seq assay as well as coherently down-regulated targets of other coherently up-regulated miRs beyond *ame-miR-375-3p* between Q-Mdg and QLW-Mdg.

Concluding Remarks

Here we identified robust miR expression profiles by caste and by social status in the honey bee MG as well as the cognate target down-regulated genes by expression context. We provide computational and functional evidence suggesting the queen-less bee phenotype results from down-regulating worker-expressed genes via up-regulating a sub-set of queen-expressed miRs. We also show the importance of context when evaluating the role of taxonomically-restricted miRs in the evolution of new traits and suggest more recently derived tissues may be focal points of subsequent study. In addition to more detailed functional analysis and validation of predicted

targets, future studies should explore the role of novel miRs more broadly across multiple tissue types and, perhaps, with a focus on novel cell types.

Materials and methods

Honey Bee Field Work and Sample Selection

All work with honey bees was conducted at the Harry H. Laidlaw Jr. Honey Bee Research Facility at University of California Davis (Davis, CA) primarily in the summer of 2015. Multiple queens were grafted from three single drone inseminated (SDI) queens in order to reduce genetic variation using established techniques [149]. In a haplodiploid context, the daughters of single-drone inseminated queens are known as “super-sisters” as they have a coefficient of relatedness (G) of 0.75. Early worker larvae were placed in plastic queen-cups containing freshly collected royal jelly and reared in specialized queen-less colonies as previously described [149]. Sealed queen cells were then placed in an incubator for 48 hours at 34°C and 60% relative humidity and then introduced into temporary nucleus hives with approximately 10000 workers from the same parent colony, a brood frame, a frame with both pollen and honey, and an empty frame [150]. The queens were then either allowed to mate freely until the first observation of egg laying or queen cells were prevented from mating. Queens and newly emerged workers from the same parent colony were then placed into in micro-hives modeled after a previous study [27] and maintained in an incubator (34°C, 60% r.h.). Briefly, plastic hives (11×14×7 cm, H×L×W) were constructed, a small comb was affixed to the ceiling, and a small

amount of pollen cake was provided, and sugar solution was provided ad libitum. Experimental micro-hive subsets constructed as follows: from each of the three SDI parent hives; five virgin queens each with 50 newly emerged workers, five mated queens each with 50 newly emerged workers, five sets 50 newly emerged workers from the same SDI parent colony with an established queen (“queen-right” workers) so as to avoid any possible confounding effects of using experimental queens with experimental workers, and five sets of 50 newly emerged workers with no queen (“queen-less” workers). All virgin and mated queens and subsets of workers were collected at three weeks of age to control for age effects and directly placed in a freezer at -80°C where they remained until sample processing.

In order to evaluate the relationship between miR expression in the mandibular gland and ovary development, the ovary development level of individual queen-less worker bees was assessed prior to mandibular gland miR expression analysis. To maintain RNA integrity in the Mdg, queen-less worker heads and abdomens were separated from the body on dry ice and placed into separate containers of RNA-Later ICE (Thermo-Fisher Scientific) and placed in a -20°C freezer according to manufacturer instructions. Abdomens were then dissected by cutting a square out of the dorsal cuticle, removing the alimentary canal [151], and the ovary activation level was evaluated using a protocol modified from a previous study [152] where stage zero is an ovary with no observed activation, stage one is ovary enlargement with no observable oocyte development, stage two is some oocyte development, and stage three is fully developed eggs. Ovaries advanced beyond stage

one were considered “developed”. Mandibular glands and fat body tissue were then dissected by removing the samples from RNA later ICE and then dissected as previously described [113].

MicroRNA sequencing

Total RNA was extracted from individual bees using Direct-zol RNA extraction kit (Zymo Research) with the optional DNase I step included. RNA purity was assessed using a Nanodrop Spectrophotometer (Thermo Fisher Scientific), concentrations were assessed using Qubit (Thermo Fisher Scientific), and RNA quality was assessed using Experion RNA HighSens Analysis Kits (Bio-Rad). Small RNA Sequencing libraries were made using NEXTflex Small RNA-Seq Kit v3 (BIOO Scientific Corp.) in accordance with manufacturer protocols. This kit was selected because of reports that its’ use of randomized sequence primers leads to reduction in bias and compartment with RT-qPCR expression analysis [153,154]. Libraries were sequenced at the UC Davis Genome Center on the Illumina HiSEQ 4000 with single read sequencing for 50 cycles. Sequencing quality was assessed using FastQC [155] and Cutadapt [156] was used to remove BIOO adapter sequences and return reads with a minimum length of 25 nucleotides. Fastx trimmer was then used to remove the four random bases the BIOO library kit adds flanking each end of the read sequence [157]. Prior to differential expression analysis, novel miRNAs with a score of greater than or equal to five were identified using miRDeep2 [158,159]. Reads with a minimum length of 18 nucleotides were then mapped to the *A.mel* genome (version

HAv3.1) using the “mapper” program in the miRDeep2 program suite [158–160]. The current set of *A.mel* mature and hairpin miRNA sequences were obtained from miRbase in fasta format [161]. Spaces were removed from headers of the miRbase *A.mel* microRNA fasta files as well as the genome fasta reference file in order to be readable by miRDeep2. A report of all detected miRNAs is generated by miRDeep2, including putative novel miRNAs which are given a score. Read counts were then generated using the “quantifier” program in the miRDeep2 program suite for known *A.mel* miRNAs and putative novel miRNA sequences with a miRDeep2 score of ≥ 5 [158]. The differential expression of miRNAs across multiple pairwise comparisons (decide test table) was assessed using the limmavoom program using a cutoff of ≤ 0.05 for false discovery rate, 173 very lowly expressed miRNAs out of 362 were filtered using “filterByExpr”, and libraries were normalized using the trimmed mean of M-values (TMM) method [162]. A multi-dimensional scaling (MDS) plot of the samples (Fig 1A) was generated where distance between the samples is inversely proportional to the similarity of expression profiles [162]. The most dynamically expressed miRNAs (miRNAs with both mean counts-per-million and expression variance values ≥ 50) were placed in a heatmap of expression clusters by centering and scaling expression data where samples (columns) were clustered via the spearman correlation method and rows (miRNA) were clustered via the pearson correlation method (Fig 1C) [163,164]. The sum of squared error, average silhouette width, and the Calinski criterion method of determining the optimal number of expression clusters, all determined that the optimal number of clusters for k-means clustering

was three [163,164]. Each of the most dynamically expressed miRNA was then assigned to one of three clusters using k-means clustering. The correlation of each experimental group to each cluster was calculated using a student t-test (Fig 1B) [163,164].

MicroRNA Target Prediction

Three programs were used to predict microRNA response elements (MREs) within the latest *A.mel* transcriptome assembly [160]. Fasta sequences for established miRNA were obtained from the miRbase.org repository supplemented with predicted novel sequences [161]. RNA22v2 [165] was run with a threshold of minimum free energy (mfe) -12.0 kcal/mol, RNAHybrid [166] with a mfe threshold of -20.0 kcal/mmol with the xi and theta values estimated using the fly (*Drosophila melanogaster*) 3' UTR set, and miRanda3.0 also with a minimum free energy threshold of -20.0 kcal/mmol and a minimum score threshold of 140 [167]. An MRE was kept if it was predicted by at least two out of three programs and if the 3' end was within a maximum range of 5 nucleotides. The location of the MRE relative to the coding sequence, whether in the 5' untranslated region (UTR), the coding sequence (CDS) itself, or the 3' UTR, was determined using NCBI CDS coordinates. While questions remain about the translation inhibition efficiency of non-canonical MREs [168], they were included in this analysis given the multiple lines of evidence suggesting functionality [169–174]. For each predicted gene-miRNA target pair, a MRE-per transcript-per-gene metric was calculated by dividing the number of MREs by the

number of transcripts within a gene. Each target pair was also searched for corresponding validation amongst two *Drosophila melanogaster* data sources, crosslinking and immunoprecipitation (CLIP) data [168] and predicted target (TARGETSCAN) data [175]. Corresponding orthologous genes as well as taxonomic restriction level (Table S17) for each *A.mel* gene were determined using OrthoDB v10 [176] which generates clusters of orthologous inter-species gene pairings using the best reciprocal hits method. Genes or miRs were considered “novel” if they were restricted to *Hymenoptera*. Genes with a OrthoDB gene ID but without an OrthoDB unique ID were considered unique to *A.mel*. We used hypergeometric tests (Table S13) to evaluate enrichment of categories of MREs within sets of genes expressed according to caste or mating status in the Mdg [14,177]. We tested for enrichment of individual miR or groupings of MREs within all MREs in groupings of genes expressed according to either caste or mating status relative to the proportion of all MREs for that selection of miRs amongst all MREs of all genes. The expected number of MREs in any of the categories was calculated by taking the product of MREs for those same miRs within the select list of genes and the total number of MREs for the select miRs within all transcripts and dividing by the total number of MREs within all genes. Fold change enrichment was calculated by dividing the observed number of MREs by the expected. Enrichment p-values were calculated using a cumulative distribution function of the hypergeometric distribution [14,177].

Systems Analysis / mPPI networks

We generated four putative microRNA-protein-protein interaction (mPPI) networks composed of anti-correlated pairings of miRs up-regulated in the mandibular gland with respect to either caste (queens and queen-right workers) or mating status (queen-right workers and queen-less workers) and their cognate predicted targets amongst genes down-regulated in the same context. Gene expression data was taken from previously published mandibular gland RNA-Seq data [14]. Orthologs were identified for each predicted target gene using OrthoDB v 10.0 [176] as previously described. Sub-network sets of predicted anti-correlated target orthologs were filtered from the *Drosophila* BioGRID-3.5.186 network dataset [68] in Cytoscape v3.8 [182]. Each mPPI included first-degree neighbor proteins whose *A. mel* orthologs are also predicted to be targeted by at least one anti-correlated miR. Target predictions were imported to each mPPI as edge data and distinguished visually as “predicted” or as being validated by CLIP and/or TARGETSCAN in *Drosophila melanogaster*. For this analysis, we ignored the total number of times a miR is predicted to target a transcript. Gene ontology (GO) functional analysis (biological process) was conducted using the ClueGO plugin v2.5.7 [183] for each of the four mPPIs, any miR target subset of 115 targets or more, and the subsets of coherent targets between queen-less workers and queens with respect to expression direction. The GO term fusion option was selected, p values were obtained using Fisher Exact Test and were corrected via Bonferroni step down. This basic approach was taken from another study [184] with modifications. The most highly targeted DEGs, representing the top 20% of total MREs amongst DEGs with a *D. melanogaster* ortholog, were also assessed for

functional categorization and statistical overrepresentation using PANTHER with default settings [185]. To more deeply assess the influence of individual miRs in regulating expression, anti-correlated miR expression and target data were integrated by taking the log of the product of the average categorical counts per million (CPM) of each miR and the total number of its' predicted down-regulated targets within the DEG list [14]. There was no substantive difference between total MREs/miR or total targets/miR.

Network topological analysis of each of the miR-specific sub-mPPIs networks was conducted by comparing the average degree, average number of neighbors, characteristic path length, clustering coefficient, and network density to that of random genes selected from the full *D. melanogaster* BioGRID dataset. Sets of 100 random genes were compared to the predicted target gene set of each miR. The non-parametric Kolmogorov–Smirnov test was used to test the assumption that miR-specific mPPIs networks were comprised of random connections.

Another protein-protein interaction (PPI) sub-network of the *D. melanogaster* BioGRID dataset without first-degree proteins was curated from genes differentially-expressed in the mandibular gland of bees fed an antagomir relative to controls. The same topological and functional analyses were conducted on this PPI as described above.

3' TAG-Seq of Bees fed MiRNA Inhibitors

Antagomirs, synthetic RNA oligonucleotides exactly complementary to mature miRNAs, inhibit target microRNA *in vivo*. Queen-less bees from three SDI parent colonies were fed custom miRCURY LNA cholesterol-conjugated antagomirs for ame-miR-7-5p and ame-miR-375-3p (Qiagen) diluted to 1 μ g/ μ l in a sugar solution, in addition to a scrambled control sequence and a sugar-only control treatment [184]. Approximately fifty age-controlled newly emerged bees per SDI colony per treatment were kept in micro-hives and maintained as previously described. On the twentieth day, bees were chilled and harnessed using Eppendorf tubes with sawed-off tips and ~3.5 cm straw inserts [186,187]. The bees were then placed in an incubator for 20 minutes and then kept at room temperature for 10 minutes before feeding. The bees were fed one microliter of either sugar control, scrambled control, anti-ame-miR-7-5p, or anti-ame-miR-375-3p, returned to their micro-hives, returned to the incubator for an additional 24 hours, and subsequently placed directly into the -80°C freezer. Individual mandibular glands were dissected from three individuals from each group and each of the three biological replicates for a total of thirty-six samples. Dissections and RNA extractions were conducted as described above. Custom 3' TAG-Seq libraries were prepared at the DNA Technologies Core of the UC Davis Genome Center and sequenced on the Illumina HiSeq 4000. Adapters were removed from the raw reads using Cutadapt. Reads were aligned to the latest version (HAV3.1) of the *A.mel* genome using the STAR aligner using default settings with the --sjdbGTFtagExonParentGene option set to "gene". Htseq-count was used to generate counts with the -m union option and the "id attribute" and "feature type" set to "gene".

Htseq-count was repeated with the “feature type” set to “pseudogene”. Output files were combined into table format and assessed for differential expression between groups using limmavoom as above. Taxonomic restriction for each gene was inferred using the “OGid” from OrthoDB v10 [176] with the lowest taxonomic identifier. It is assumed here that genes without an OGid are unique to *A.mel*.

Supporting Information

Table S1: The average number of aligned reads per sample was approximately 3.5 million with a standard deviation of 2.2 million reads and a minimum of one million reads and a maximum of ten million. (.xlsx)

Table S2: Pairwise comparisons were conducted across multiple experimental groups. (.xlsx)

Table S3: Limma zoom calculations of significantly differentially-expressed miRs. The data is tabbed where individual comparisons between groups are located on unique tabs. Also included is a list of miRs coherently expressed in terms of direction between queens and queen-right workers (QRWs) in both the Mdg and FB, logFC values of coherent DE-miRs, average expression in both tissues, the absolute value of the log difference in expression between queens and QRW in both tissues, log2 fold change in average expression across tissues with respect to caste, and a note where expression represents the highest percentage of overall expression by caste. Log(abs)

was not calculated for all comparisons. Note that “W” stands for all worker groups (QRW, QLU, & QLD) together as a single group. (.xlsx)

Table S4: Counts per million values of each miR in each sample. Average CPM was calculated by group. The absolute values of the log differences in expression between groups was also calculated. (.xlsx)

Table S5: Network analysis data for full mPPI networks. “QvW” is miRs up-regulated and genes down-regulated in queens versus queen-right workers. “WvQ” is miRs up-regulated and genes down-regulated in queen-right workers versus queens. “QLWvQRW” is miRs up-regulated and genes down-regulated in queen-less workers versus queen-right workers. “QRWvQLW” is miRs up-regulated and genes down-regulated in queen-right workers versus queen-less workers. (.xlsx)

Table S6: Network analysis data for full mPPI networks. Each tab lists network analysis data the target networks of individual DE-miRs up-regulated in that context as well as any significant associated GO terms representing 5% or more of network nodes. Tab names are the same as in Table S5 but also include “DQW_DQLQR” and “DWQ_DQRQL” which are anti-correlated target pairs in common between “DQW” and “QLWvQRW” as well as “DWQ” and “QRWvQLW” respectively. (.xlsx)

Table S7: Target data for 49 DEGs. “miRs/gene” represents the number of individual miRs predicted to target a DEG. “MREs/gene” represents the total number of MREs predicted on a gene. “Top 20% of targets” represents if a gene is in the top 20% of MREs/gene. Tabs are labeled as in Table S5. (.xlsx)

Table S8: Edge data for all mPPI networks. Tabs are labeled as in Table S5. (.xlsx)

Table S9: TAG-Seq limma zoom data including supplemental information. If a gene increased in expression in antagomir-fed bees relative to queen-less control bees, and that gene was also higher in expression in queen-right workers relative to queen-less workers or queens, it was designated “QR-like-vQL” and/or “QRW-like-vQ” respectively. In the columns “Yang et al., 2017 10-HDA Proteome” and “Begna et al., 2011 Q/W Larvae Proteome”, the gene’s accession number is listed if the protein of the gene was found in proteome data of the respective paper. Protein categories from 52 and gene expression data from 49 are included. Log2 differences in expression values were calculated for 49 as well as control (con) and experimental (A375) bees. “A375” and “con” are shorthand for antagomir-fed bees and control queen-less bees respectively. “MREs/transcript/gene” is an average value of MREs per transcript per gene. The column “DQvQRW-QLvQRW” lists the gene’s accession number if the gene is coherently regulated in queens and queen-less bees with respect to queen-right workers. Most recent ortholog between *Drosophila melanogaster* and *Apis mellifera*

as well as the level of taxonomic restriction of each *Apis mellifera* gene are listed.
(.xlsx)

Table S10: Coherent down-regulated DEGS in queens and queen-less worker mandibular glands relative to worker mandibular glands via transcription data from 49. (.xlsx)

Table S11: Target data of coherently regulated genes from Table S10. Mandibular gland expression data taken from 49. As calculations of log₂ fold change (LogFC) do not quantify the absolute change in expression values, we also calculated the log values of the absolute differences between the average RPKM values for each gene to quantify the change in percent total expression. “QLvQRW” is queen-less workers versus queen-right workers. “QvQRW” is queens versus queen-right workers. (.xlsx)

Table S12: Ratio of percent expression of novel and conserved genes (defined as genes found either within or conserved beyond Hymenoptera) divided by the number of novel or conserved genes respectively from transcription data from 49. If the ratio is greater than one, that category of gene represents a positive disproportion of expression relative to the number of genes expressed. (.xlsx)

Table S13: Enrichment of individual DE-miR MREs within anti-correlated predicted target genes for each comparison. Tabs are labeled as in Table S5. (.xlsx)

Table S14: Putative Pheromone Biosynthesis Genes. Listed are the predicted steps in the biosynthesis of fatty acid pheromones, expression data from previous studies [8,14] and predicted MREs for each PPBG. (.xlsx)

Table S15: Network analysis of genes differentially-expressed between queen-less bees fed an antagomir for ame-miR-375-3p and control queen-less bees. Network analysis conducted the same as in Table S6 (.xlsx)

Table S16: Novel miRs determined by miRdeep2 [158,159] (.xlsx)

Table S17: OrthoDB [176] IDs and information for each *Apis mellifera* gene. (.xlsx)

Acknowledgements

We thank Joanna Chiu and Siobhan Brady for manuscript comments and advice. We thank members of Chiu lab at UC Davis; Antoine Abrieux, Xian-Hui (Nitrol) Liu, Yao Cai, Christine Tabuloc, Rosanna Kwok, Vu Lam, and Ying Li, for advice, training on methodology, and access to lab equipment. We thank Osnat Malka of Hebrew University of Jerusalem for advice on micro-hive construction. We thank Kaisa Kajala of the Brady lab at UC Davis for advice on experimental design. We thank Christopher Pagan of the Steve Nadler lab at UC Davis for advice on concepts and

implementation. We thank Amy Michaud of the Caswell-Chen lab of the for help with implementation. We thank Geoffrey Attardo for advice on methodology and for access to lab equipment. We thank Lutz Froenicke, Oanh Nguyen, and Vanessa Rashbrook of the UC Davis Genome Center for advice and assistance on high-throughput sequencing. We thank Monica Britton and Matt Settles of the UC Davis Bioinformatics Core for advice on experimental design and reviewing bioinformatic pipelines. We thank Bernardo Niño and Charley Nye of the Harry H. Laidlaw Jr. Honey Bee Research Facility for help with honey bee hive training, maintenance, and implementation.

Author Contributions

Conceptualization: W. Cameron Jasper, Elina L. Niño.

Data curation: W. Cameron Jasper.

Formal analysis: W. Cameron Jasper.

Funding acquisition: W. Cameron Jasper, Elina L. Niño.

Investigation: W. Cameron Jasper.

Methodology: W. Cameron Jasper.

Project administration: W. Cameron Jasper, Elina L. Niño.

Resources: Elina L. Niño.

Software: W. Cameron Jasper.

Supervision: Elina L. Niño.

Validation: W. Cameron Jasper.

Visualization: W. Cameron Jasper.

Writing – original draft: W. Cameron Jasper.

Writing – review & editing: W. Cameron Jasper, Elina L. Niño.

References

1. Winston ML. The Biology of the Honey Bee. Harvard University Press; 1991.
2. Bortolotti L, Costa C. Chemical Communication in the Honey Bee Society. In: C M-C, editor. Neurobiology of Chemical Communication. 2014.
3. Slessor KN, Winston ML, Conte YL. Pheromone Communication in the Honeybee (*Apis mellifera* L.). *J Chem Ecol.* 2005;31: 2731–2745. doi:10.1007/s10886-005-7623-9
4. Plettner E, Slessor KN, Winston ML, Oliver JE. Caste-Selective Pheromone Biosynthesis in Honeybees. *Science.* 1996;271: 1851–1853. doi:10.1126/science.271.5257.1851
5. Pankiw T, Huang Z- Y, Winston ML, Robinson GE. Queen mandibular gland pheromone influences worker honey bee (*Apis mellifera* L.) foraging ontogeny and juvenile hormone titers. *J Insect Physiol.* 1998;44: 685–692. doi:10.1016/s0022-1910(98)00040-7
6. Buttstedt A, Ihling CH, Pietzsch M, Moritz RFA. Royalactin is not a royal making of a queen. *Nature.* 2016;537: E10–E12. doi:10.1038/nature19349
7. Rangel J, Böröczky K, Schal C, Tarpy DR. Honey Bee (*Apis mellifera*) Queen Reproductive Potential Affects Queen Mandibular Gland Pheromone Composition and Worker Retinue Response. Nascimento FS, editor. *Plos One.* 2016;11: e0156027. doi:10.1371/journal.pone.0156027
8. Malka O, Niño EL, Grozinger CM, Hefetz A. Genomic analysis of the interactions between social environment and social communication systems in honey bees (*Apis mellifera*). *Insect Biochem Molec.* 2014;47: 36–45. doi:10.1016/j.ibmb.2014.01.001
9. Niño EL, Malka O, Hefetz A, Tarpy DR, Grozinger CM. Chemical Profiles of Two Pheromone Glands Are Differentially Regulated by Distinct Mating Factors in Honey Bee Queens (*Apis mellifera* L.). Chaline N, editor. *Plos One.* 2013;8: e78637. doi:10.1371/journal.pone.0078637

10. Kocher SD, Richard F-J, Tarpy DR, Grozinger CM. Queen reproductive state modulates pheromone production and queen-worker interactions in honeybees. *Behav Ecol.* 2009;20: 1007–1014. doi:10.1093/beheco/arp090
11. Kocher SD, Richard F-J, Tarpy DR, Grozinger CM. Genomic analysis of post-mating changes in the honey bee queen (*Apis mellifera*). *Bmc Genomics.* 2008;9: 232–232. doi:10.1186/1471-2164-9-232
12. Slessor KN, Kaminski L-A, King GGS, Winston ML. Semiochemicals of the honeybee queen mandibular glands. *J Chem Ecol.* 1990;16: 851–860. doi:10.1007/bf01016495
13. Naumann K, Winston ML, Slessor KN, Prestwich GD, Webster FX. Production and transmission of honey bee queen (*Apis mellifera* L.) mandibular gland pheromone. *Behav Ecol Sociobiol.* 1991;29: 321–332. doi:10.1007/bf00165956
14. Wu Y, Zheng H, Corona M, Pirk C, Meng F, Zheng Y, et al. Comparative transcriptome analysis on the synthesis pathway of honey bee (*Apis mellifera*) mandibular gland secretions. *Sci Rep-uk.* 2017;7: 4530. doi:10.1038/s41598-017-04879-z
15. Vallet A, Cassier P, Lensky Y. Ontogeny of the fine structure of the mandibular glands of the honeybee (*Apis mellifera* L.) workers and the pheromonal activity of 2-heptanone. *J Insect Physiol.* 1991;37: 789–804. doi:10.1016/0022-1910(91)90076-c
16. Snodgrass R. *Anatomy of the Honey Bee.* Ithaca, York N, editors. Ithaca, New York: Comstock Publ. Assoc; 1956.
17. Yang X-H, Yang S-F, Wang R-M. Comparative proteomic analysis provides insight into 10-hydroxy-2-decenoic acid biosynthesis in honey bee workers. *Amino Acids.* 2017;49: 1177–1192. doi:10.1007/s00726-017-2418-1
18. Yusuf AA, Pirk CWW, Crewe RM. Mandibular gland pheromone contents in workers and queens of *Apis mellifera adansonii*. *Apidologie.* 2015;46: 559–572. doi:10.1007/s13592-014-0346-6
19. BARKER SA, FOSTER AB, LAMB DC, HODGSON N. Identification of 10-Hydroxy- Δ^2 -decenoic Acid in Royal Jelly. *Nature.* 1959;183: 996–997. doi:10.1038/183996a0
20. Yang Y-C, Chou W-M, Widowati DA, Lin I-P, Peng C-C. 10-hydroxy-2-decenoic acid of royal jelly exhibits bactericide and anti-inflammatory activity in human colon cancer cells. *Bmc Complem Altern M.* 2018;18: 202. doi:10.1186/s12906-018-2267-9
21. Spannhoff A, Kim YK, Raynal NJ - M, Gharibyan V, Su M, Zhou Y, et al. Histone deacetylase inhibitor activity in royal jelly might facilitate caste switching in bees. *Embo Rep.* 2011;12: 238–243. doi:10.1038/embor.2011.9

22. Papachristoforou A, Kagiava A, Papaefthimiou C, Termentzi A, Fokialakis N, Skaltsounis A-L, et al. The Bite of the Honeybee: 2-Heptanone Secreted from Honeybee Mandibles during a Bite Acts as a Local Anaesthetic in Insects and Mammals. Skoulakis EMC, editor. Plos One. 2012;7: e47432. doi:10.1371/journal.pone.0047432
23. De-Hazan M, Hyams J, Lensky Y, Cassier P. Ultrastructure and ontogeny of the mandibular glands of the queen honey bee, *Apis mellifera* L. (Hymenoptera: Apidae). *Int J Insect Morphol Embryology*. 1989;18: 311–320. doi:10.1016/0020-7322(89)90012-3
24. Wu Y, Zheng Y, Li-Byarlay H, Shi Y, Wang S, Zheng H, et al. CYP6AS8, a cytochrome P450, is associated with the 10-HDA biosynthesis in honey bee (*Apis mellifera*) workers. *Apidologie*. 2020;51: 1202–1212. doi:10.1007/s13592-019-00709-5
25. Malka O, Karunker I, Yeheskel A, Morin S, Hefetz A. The gene road to royalty – differential expression of hydroxylating genes in the mandibular glands of the honeybee. *Febs J*. 2009;276: 5481–5490. doi:10.1111/j.1742-4658.2009.07232.x
26. Plettner E, Slessor KN, Winston ML. Biosynthesis of Mandibular Acids in Honey Bees (*Apis mellifera*): De novo Synthesis, Route of Fatty Acid Hydroxylation and Caste Selective β -Oxidation. *Insect Biochem Molec*. 1998;28: 31–42. doi:10.1016/s0965-1748(97)00079-9
27. Malka O, Shnieor S, Hefetz A, Katzav-Gozansky T. Reversible royalty in worker honeybees (*Apis mellifera*) under the queen influence. *Behav Ecol Sociobiol*. 2006;61: 465–473. doi:10.1007/s00265-006-0274-1
28. Plettner E, Slessor KN, Winston ML, Robinson GE, Page RE. Mandibular gland components and ovarian development as measures of caste differentiation in the honey bee (*Apis mellifera* L.). *J Insect Physiol*. 1993;39: 235–240. doi:10.1016/0022-1910(93)90094-8
29. Crewe RM, Velthuis HHW. False queens: A consequence of mandibular gland signals in worker honeybees. *Naturwissenschaften*. 1980;67: 467–469. doi:10.1007/bf00405650
30. Huang Z-Y, Robinson GE. Regulation of honey bee division of labor by colony age demography. *Behav Ecol Sociobiol*. 1996;39: 147–158. doi:10.1007/s002650050276
31. Robinson GE, Page RE, Strambi C, Strambi A. Colony Integration in Honey Bees: Mechanisms of Behavioral Reversion. *Ethology*. 1992;90: 336–348. doi:10.1111/j.1439-0310.1992.tb00844.x
32. Herb BR, Wolschin F, Hansen KD, Aryee MJ, Langmead B, Irizarry R, et al. Reversible switching between epigenetic states in honeybee behavioral subcastes. *Nat Neurosci*. 2012;15: 1371–1373. doi:10.1038/nn.3218
33. Wagner GP, Altenberg L. PERSPECTIVE: COMPLEX ADAPTATIONS AND THE EVOLUTION OF EVOLVABILITY. *Evolution*. 1996;50: 967–976. doi:10.1111/j.1558-5646.1996.tb02339.x

34. Wagner GP, Pavlicev M, Cheverud JM. The road to modularity. *Nat Rev Genet.* 2007;8: 921–931. doi:10.1038/nrg2267
35. Brückner A, Parker J, Dickinson MH, Vosshall LB, Dow JAT. Molecular evolution of gland cell types and chemical interactions in animals. *J Exp Biol.* 2020;223: jeb211938. doi:10.1242/jeb.211938
36. Barve A, Wagner A. A latent capacity for evolutionary innovation through exaptation in metabolic systems. *Nature.* 2013;500: 203–206. doi:10.1038/nature12301
37. Jurenka R. *The Chemistry of Pheromones and Other Semiochemicals I.* Springer Berlin Heidelberg; 2004. pp. 97–132. doi:10.1007/b95450
38. Tillman JA, Seybold SJ, Jurenka RA, Blomquist GJ. Insect pheromones--an overview of biosynthesis and endocrine regulation. *Insect Biochemistry and Molecular Biology.* 1999;29: 481–514.
39. Payne JL, Wagner A. The Robustness and Evolvability of Transcription Factor Binding Sites. *Science.* 2014;343: 875–877. doi:10.1126/science.1249046
40. Villar D, Flicek P, Odom DT. Evolution of transcription factor binding in metazoans — mechanisms and functional implications. *Nat Rev Genet.* 2014;15: 221–233. doi:10.1038/nrg3481
41. Moran Y, Agron M, Praher D, Technau U. The evolutionary origin of plant and animal microRNAs. *Nat Ecol Evol.* 2017;1: 0027. doi:10.1038/s41559-016-0027
42. Asgari S. MicroRNA functions in insects. *Insect Biochem Molec.* 2013;43: 388–397. doi:10.1016/j.ibmb.2012.10.005
43. Sun K, Lai EC. Adult-specific functions of animal microRNAs. *Nat Rev Genet.* 2013;14: 535–548. doi:10.1038/nrg3471
44. Berezikov E. Evolution of microRNA diversity and regulation in animals. *Nat Rev Genet.* 2011;12: 846–860. doi:10.1038/nrg3079
45. Heimberg AM, Sempere LF, Moy VN, Donoghue PCJ, Peterson KJ. MicroRNAs and the advent of vertebrate morphological complexity. *Proc National Acad Sci.* 2008;105: 2946–2950. doi:10.1073/pnas.0712259105
46. Chen K, Rajewsky N. The evolution of gene regulation by transcription factors and microRNAs. *Nat Rev Genet.* 2007;8: 93–103. doi:10.1038/nrg1990
47. Bartel DP. Metazoan MicroRNAs. *Cell.* 2018;173: 20–51. doi:10.1016/j.cell.2018.03.006

48. Ebert MS, Sharp PA. Roles for MicroRNAs in Conferring Robustness to Biological Processes. *Cell*. 2012;149: 515–524. doi:10.1016/j.cell.2012.04.005
49. Lee C-T, Risom T, Strauss WM. Evolutionary Conservation of MicroRNA Regulatory Circuits: An Examination of MicroRNA Gene Complexity and Conserved MicroRNA-Target Interactions through Metazoan Phylogeny. *Dna Cell Biol*. 2007;26: 209–218. doi:10.1089/dna.2006.0545
50. Kehl T, Backes C, Kern F, Fehlmann T, Ludwig N, Meese E, et al. About miRNAs, miRNA seeds, target genes and target pathways. *Oncotarget*. 2017;8: 107167–107175. doi:10.18632/oncotarget.22363
51. Bracken CP, Scott HS, Goodall GJ. A network-biology perspective of microRNA function and dysfunction in cancer. *Nat Rev Genet*. 2016;17: 719–732. doi:10.1038/nrg.2016.134
52. Tibiche C, Wang E. MicroRNA Regulatory Patterns on the Human Metabolic Network. *Open Syst Biology J*. 2008;1: 1–8. doi:10.2174/1876392800801010001
53. Wang S, Adams KL. Duplicate Gene Divergence by Changes in MicroRNA Binding Sites in Arabidopsis and Brassica. *Genome Biol Evol*. 2015;7: 646–655. doi:10.1093/gbe/evv023
54. Li J, Musso G, Zhang Z. Preferential regulation of duplicated genes by microRNAs in mammals. *Genome Biol*. 2008;9: R132. doi:10.1186/gb-2008-9-8-r132
55. Turetzek N, Pechmann M, Schomburg C, Schneider J, Prpic N-M. Neofunctionalization of a Duplicate *dachshund* Gene Underlies the Evolution of a Novel Leg Segment in Arachnids. *Mol Biol Evol*. 2016;33: 109–121. doi:10.1093/molbev/msv200
56. Zattara EE, Busey HA, Linz DM, Tomoyasu Y, Moczek AP. Neofunctionalization of embryonic head patterning genes facilitates the positioning of novel traits on the dorsal head of adult beetles. *Proc Royal Soc B Biological Sci*. 2016;283: 20160824. doi:10.1098/rspb.2016.0824
57. Assis R, Bachtrog D. Neofunctionalization of young duplicate genes in *Drosophila*. *Proc National Acad Sci*. 2013;110: 17409–17414. doi:10.1073/pnas.1313759110
58. Prochnik SE, Rokhsar DS, Aboobaker AA. Evidence for a microRNA expansion in the bilaterian ancestor. *Dev Genes Evol*. 2006;217: 73–77. doi:10.1007/s00427-006-0116-1
59. Davidson EH, Erwin DH. Gene Regulatory Networks and the Evolution of Animal Body Plans. *Science*. 2006;311: 796–800. doi:10.1126/science.1113832
60. Sempere LF, Cole CN, Mcpeek MA, Peterson KJ. The phylogenetic distribution of metazoan microRNAs: insights into evolutionary complexity and constraint. *J Exp Zoology Part B Mol Dev Evol*. 2006;306B: 575–588. doi:10.1002/jez.b.21118

61. Peláez N, Carthew RW. Chapter nine Biological Robustness and the Role of MicroRNAs A Network Perspective. Elsevier; 2012. pp. 237–255. doi:10.1016/b978-0-12-387038-4.00009-4
62. Peterson KJ, Dietrich MR, McPeck MA. MicroRNAs and metazoan macroevolution: insights into canalization, complexity, and the Cambrian explosion. *Bioessays*. 2009;31: 736–747. doi:10.1002/bies.200900033
63. Berkhout J, Teusink B, Bruggeman FJ. Gene network requirements for regulation of metabolic gene expression to a desired state. *Sci Rep-uk*. 2013;3: 1417. doi:10.1038/srep01417
64. Rottiers V, Näär AM. MicroRNAs in metabolism and metabolic disorders. *Nat Rev Mol Cell Bio*. 2012;13: 239–250. doi:10.1038/nrm3313
65. Fernández-Hernando C, Suárez Y, Rayner KJ, Moore KJ. MicroRNAs in lipid metabolism. *Curr Opin Lipidol*. 2011;22: 86–92. doi:10.1097/mol.0b013e3283428d9d
66. Krützfeldt J, Stoffel M. MicroRNAs: A new class of regulatory genes affecting metabolism. *Cell Metab*. 2006;4: 9–12. doi:10.1016/j.cmet.2006.05.009
67. Harpur BA, Kent CF, Molodtsova D, Lebon JMD, Alqarni AS, Owayss AA, et al. Population genomics of the honey bee reveals strong signatures of positive selection on worker traits. *Proc National Acad Sci*. 2014;111: 2614–2619. doi:10.1073/pnas.1315506111
68. Oughtred R, Stark C, Breitkreutz B-J, Rust J, Boucher L, Chang C, et al. The BioGRID interaction database: 2019 update. *Nucleic Acids Res*. 2019;47: D529–D541. doi:10.1093/nar/gky1079
69. Salunkhe VA, Esguerra JLS, Ofori JK, Mollet IG, Braun M, Stoffel M, et al. Modulation of micro RNA - 375 expression alters voltage - gated Na + channel properties and exocytosis in insulin - secreting cells. *Acta Physiol*. 2015;213: 882–892. doi:10.1111/apha.12460
70. Erener S, Mojibian M, Fox JK, Denroche HC, Kieffer TJ. Circulating miR-375 as a Biomarker of β -Cell Death and Diabetes in Mice. *Endocrinology*. 2013;154: 603–608. doi:10.1210/en.2012-1744
71. Li Y, Xu X, Liang Y, Liu S, Xiao H, Li F, et al. miR-375 enhances palmitate-induced lipoapoptosis in insulin-secreting NIT-1 cells by repressing myotrophin (V1) protein expression. *Int J Clin Exp Patho*. 2010;3: 254–64.
72. Baroukh NN, Obberghen EV. Function of microRNA - 375 and microRNA - 124a in pancreas and brain. *Febs J*. 2009;276: 6509–6521. doi:10.1111/j.1742-4658.2009.07353.x
73. Higuchi C, Nakatsuka A, Eguchi J, Teshigawara S, Kanzaki M, Katayama A, et al. Identification of Circulating miR-101, miR-375 and miR-802 as Biomarkers for Type 2 Diabetes. *Metabolis*. 2015;64: 489–497. doi:10.1016/j.metabol.2014.12.003

74. Huang X, Yuan T, Liang M, Du M, Xia S, Dittmar R, et al. Exosomal miR-1290 and miR-375 as Prognostic Markers in Castration-resistant Prostate Cancer. *Eur Urol*. 2015;67: 33–41. doi:10.1016/j.eururo.2014.07.035
75. Poy MN, Hausser J, Trajkovski M, Braun M, Collins S, Rorsman P, et al. miR-375 maintains normal pancreatic α - and β -cell mass. *Proc National Acad Sci*. 2009;106: 5813–5818. doi:10.1073/pnas.0810550106
76. Lynn FC. Meta-regulation: microRNA regulation of glucose and lipid metabolism. *Trends Endocrinol Metabolism*. 2009;20: 452–459. doi:10.1016/j.tem.2009.05.007
77. Ouaamari AE, Baroukh N, Martens GA, Lebrun P, Pipeleers D, Obberghen E van. miR-375 Targets 3' -Phosphoinositide-Dependent Protein Kinase-1 and Regulates Glucose-Induced Biological Responses in Pancreatic β -Cells. *Diabetes*. 2008;57: 2708–2717. doi:10.2337/db07-1614
78. Lovis P, Gattesco S, Regazzi R. Regulation of the expression of components of the exocytotic machinery of insulin-secreting cells by microRNAs. *Biol Chem*. 2008;389: 305–312. doi:10.1515/bc.2008.026
79. Kloosterman WP, Lagendijk AK, Ketting RF, Moulton JD, Plasterk RHA. Targeted Inhibition of miRNA Maturation with Morpholinos Reveals a Role for miR-375 in Pancreatic Islet Development. Carrington JC, editor. *Plos Biol*. 2007;5: e203. doi:10.1371/journal.pbio.0050203
80. Poy MN, Eliasson L, Krutzfeldt J, Kuwajima S, Ma X, MacDonald PE, et al. A pancreatic islet-specific microRNA regulates insulin secretion. *Nature*. 2004;432: 226–230. doi:10.1038/nature03076
81. Hyun S, Lee JH, Jin H, Nam J, Namkoong B, Lee G, et al. Conserved MicroRNA miR-8/miR-200 and Its Target USH/FOG2 Control Growth by Regulating PI3K. *Cell*. 2009;139: 1096–1108. doi:10.1016/j.cell.2009.11.020
82. Fossett N, Zhang Q, Gajewski K, Choi CY, Kim Y, Schulz RA. The multitype zinc-finger protein U-shaped functions in heart cell specification in the *Drosophila* embryo. *Proc National Acad Sci*. 2000;97: 7348–7353. doi:10.1073/pnas.97.13.7348
83. Wei R, Yang Q, Han B, Li Y, Yao K, Yang X, et al. microRNA-375 inhibits colorectal cancer cells proliferation by downregulating JAK2/STAT3 and MAP3K8/ERK signaling pathways. *Oncotarget*. 2017;8: 16633–16641. doi:10.18632/oncotarget.15114
84. Yan J-W, Lin J-S, He X-X. The emerging role of miR-375 in cancer: The emerging role of miR-375 in cancer. *Int J Cancer*. 2013;135: 1011–1018. doi:10.1002/ijc.28563

85. Ding L, Xu Y, Zhang W, Deng Y, Si M, Du Y, et al. MiR-375 frequently downregulated in gastric cancer inhibits cell proliferation by targeting JAK2. *Cell Res.* 2010;20: 784–793. doi:10.1038/cr.2010.79
86. Chang Y, Yan W, He X, Zhang L, Li C, Huang H, et al. miR-375 Inhibits Autophagy and Reduces Viability of Hepatocellular Carcinoma Cells Under Hypoxic Conditions. *Gastroenterology.* 2012;143: 177-187.e8. doi:10.1053/j.gastro.2012.04.009
87. Ashby R, Forêt S, Searle I, Maleszka R. MicroRNAs in Honey Bee Caste Determination. *Sci Rep-uk.* 2016;6: 18794. doi:10.1038/srep18794
88. Guo X, Su S, Geir S, Li W, Li Z, Zhang S, et al. Differential expression of miRNAs related to caste differentiation in the honey bee, *Apis mellifera*. *Apidologie.* 2016;47: 495–508. doi:10.1007/s13592-015-0389-3
89. Pires CV, Freitas FC de P, Cristino AS, Dearden PK, Simões ZLP. Transcriptome Analysis of Honeybee (*Apis Mellifera*) Haploid and Diploid Embryos Reveals Early Zygotic Transcription during Cleavage. Hudson ME, editor. *Plos One.* 2016;11: e0146447. doi:10.1371/journal.pone.0146447
90. Shi Y-Y, Zheng H-J, Pan Q-Z, Wang Z-L, Zeng Z-J. Differentially expressed microRNAs between queen and worker larvae of the honey bee (*Apis mellifera*). *Apidologie.* 2014;46: 35–45. doi:10.1007/s13592-014-0299-9
91. Shi YY, Wu XB, Huang ZY, Wang ZL, Yan WY, Zeng ZJ. Epigenetic Modification of Gene Expression in Honey Bees by Heterospecific Gland Secretions. D’Esposito M, editor. *Plos One.* 2012;7: e43727. doi:10.1371/journal.pone.0043727
92. Bomtorin AD, Mackert A, Rosa GCC, Moda LM, Martins JR, Bitondi MMG, et al. Juvenile Hormone Biosynthesis Gene Expression in the corpora allata of Honey Bee (*Apis mellifera* L.) Female Castes. Korb J, editor. *Plos One.* 2014;9: e86923. doi:10.1371/journal.pone.0086923
93. Nunes FMF, Ihle KE, Mutti NS, Simões ZLP, Amdam GV. The gene vitellogenin affects microRNA regulation in honey bee (*Apis mellifera*) fat body and brain. *J Exp Biol.* 2013;216: 3724–3732. doi:10.1242/jeb.089243
94. Nelson C, Ambros V, Baehrecke EH. miR-14 Regulates Autophagy during Developmental Cell Death by Targeting ip3-kinase 2. *Mol Cell.* 2014;56: 376–388. doi:10.1016/j.molcel.2014.09.011
95. Kumarswamy R, Chandna S. Inhibition of microRNA - 14 contributes to actinomycin - D - induced apoptosis in the Sf9 insect cell line. *Cell Biol Int.* 2010;34: 851–857. doi:10.1042/cbi20100035

96. Xu P, Vernooij SY, Guo M, Hay BA. The *Drosophila* MicroRNA Mir-14 Suppresses Cell Death and Is Required for Normal Fat Metabolism. *Curr Biol.* 2003;13: 790–795. doi:10.1016/s0960-9822(03)00250-1
97. Varghese J, Lim SF, Cohen SM. *Drosophila* miR-14 regulates insulin production and metabolism through its target, sugarbabe. *Gene Dev.* 2010;24: 2748–2753. doi:10.1101/gad.1995910
98. Kania E, Roest G, Vervliet T, Parys JB, Bultynck G. IP3 Receptor-Mediated Calcium Signaling and Its Role in Autophagy in Cancer. *Frontiers Oncol.* 2017;7: 140. doi:10.3389/fonc.2017.00140
99. Decuypere J-P, Monaco G, Bultynck G, Missiaen L, Smedt HD, Parys JB. The IP3 receptor–mitochondria connection in apoptosis and autophagy. *Biochimica Et Biophysica Acta Bba - Mol Cell Res.* 2011;1813: 1003–1013. doi:10.1016/j.bbamcr.2010.11.023
100. He K, Xiao H, Sun Y, Situ G, Xi Y, Li F. microRNA-14 as an efficient suppressor to switch off ecdysone production after ecdysis in insects. *Rna Biol.* 2019;16: 1313–1325. doi:10.1080/15476286.2019.1629768
101. Liu Z, Ling L, Xu J, Zeng B, Huang Y, Shang P, et al. MicroRNA-14 regulates larval development time in *Bombyx mori*. *Insect Biochem Molec.* 2018;93: 57–65. doi:10.1016/j.ibmb.2017.12.009
102. Arbouzova NI, Bach EA, Zeidler MP. Ken & Barbie Selectively Regulates the Expression of a Subset of JAK/STAT Pathway Target Genes. *Curr Biol.* 2006;16: 80–88. doi:10.1016/j.cub.2005.11.033
103. Whitmore MM, Iparraguirre A, Kubelka L, Weninger W, Hai T, Williams BRG. Negative Regulation of TLR-Signaling Pathways by Activating Transcription Factor-3. *J Immunol.* 2007;179: 3622–3630. doi:10.4049/jimmunol.179.6.3622
104. Yan C, Lu D, Hai T, Boyd DD. Activating transcription factor 3, a stress sensor, activates p53 by blocking its ubiquitination. *Embo J.* 2005;24: 2425–2435. doi:10.1038/sj.emboj.7600712
105. Jiang H-Y, Wek SA, McGrath BC, Lu D, Hai T, Harding HP, et al. Activating Transcription Factor 3 Is Integral to the Eukaryotic Initiation Factor 2 Kinase Stress Response. *Mol Cell Biol.* 2004;24: 1365–1377. doi:10.1128/mcb.24.3.1365-1377.2004
106. Tsujino H, Kondo E, Fukuoka T, Dai Y, Tokunaga A, Miki K, et al. Activating Transcription Factor 3 (ATF3) Induction by Axotomy in Sensory and Motoneurons: A Novel Neuronal Marker of Nerve Injury. *Mol Cell Neurosci.* 2000;15: 170–182. doi:10.1006/mcne.1999.0814

107. Hartman MG, Lu D, Kim M-L, Kociba GJ, Shukri T, Buteau J, et al. Role for Activating Transcription Factor 3 in Stress-Induced β -Cell Apoptosis. *Mol Cell Biol.* 2004;24: 5721–5732. doi:10.1128/mcb.24.13.5721-5732.2004
108. Yamada A, Pang K, Martindale MQ, Tochinai S. Surprisingly complex T - box gene complement in diploblastic metazoans. *Evol Dev.* 2007;9: 220–230. doi:10.1111/j.1525-142x.2007.00154.x
109. Jennings BH, Ish-Horowicz D. The Groucho/TLE/Grg family of transcriptional co-repressors. *Genome Biol.* 2008;9: 205. doi:10.1186/gb-2008-9-1-205
110. Ditch LM, Shirangi T, Pitman JL, Latham KL, Finley KD, Edeen PT, et al. *Drosophila* retained/dead ringer is necessary for neuronal pathfinding, female receptivity and repression of fruitless-independent male courtship behaviors. *Development.* 2004;132: 155–164. doi:10.1242/dev.01568
111. Gregory SL, Kortschak RD, Kalionis B, Saint R. Characterization of the dead ringer gene identifies a novel, highly conserved family of sequence-specific DNA-binding proteins. *Mol Cell Biol.* 1996;16: 792–799. doi:10.1128/mcb.16.3.792
112. Shandala T, Takizawa K, Saint R. The dead ringer/retained transcriptional regulatory gene is required for positioning of the longitudinal glia in the *Drosophila* embryonic CNS. *Development.* 2003;130: 1505–1513. doi:10.1242/dev.00377
113. Jasper WC, Linksvayer TA, Atallah J, Friedman D, Chiu JC, Johnson BR. Large-Scale Coding Sequence Change Underlies the Evolution of Postdevelopmental Novelty in Honey Bees. *Mol Biol Evol.* 2014;32: 334–346. doi:10.1093/molbev/msu292
114. Johnson BR, Tsutsui ND. Taxonomically restricted genes are associated with the evolution of sociality in the honey bee. *Bmc Genomics.* 2011;12: 164–164. doi:10.1186/1471-2164-12-164
115. Kapheim KM, Jones BM, Søvik E, Stolle E, Waterhouse RM, Bloch G, et al. Brain microRNAs among social and solitary bees. *Roy Soc Open Sci.* 2020;7: 200517. doi:10.1098/rsos.200517
116. Li Y, Zhang R, Liu S, Donath A, Peters RS, Ware J, et al. The molecular evolutionary dynamics of oxidative phosphorylation (OXPHOS) genes in Hymenoptera. *Bmc Evol Biol.* 2017;17: 269. doi:10.1186/s12862-017-1111-z
117. Song L-R, Li D, Weng J-C, Li C-B, Wang L, Wu Z, et al. MicroRNA-195 Functions as a Tumor Suppressor by Directly Targeting Fatty Acid Synthase in Malignant Meningioma. *World Neurosurg.* 2020;136: e355–e364. doi:10.1016/j.wneu.2019.12.182
118. Sasaki R, Sur S, Cheng Q, Steele R, Ray RB. Repression of MicroRNA - 30e by Hepatitis C Virus Enhances Fatty Acid Synthesis. *Hepatology Commun.* 2019;3: 943–953. doi:10.1002/hep4.1362

119. Xu Z, Li C, Qu H, Li H, Gu Q, Xu J. MicroRNA-195 inhibits the proliferation and invasion of pancreatic cancer cells by targeting the fatty acid synthase/Wnt signaling pathway. *Tumor Biol.* 2017;39: 1010428317711324. doi:10.1177/1010428317711324
120. Lei T, Zhu Y, Jiang C, Wang Y, Fu J, Fan Z, et al. MicroRNA-320 was downregulated in non-small cell lung cancer and inhibited cell proliferation, migration and invasion by targeting fatty acid synthase. *Mol Med Rep.* 2016;14: 1255–1262. doi:10.3892/mmr.2016.5370
121. Zhao C, Tang T, Feng X, Qiu L. Cloning and characterisation of NADPH - dependent cytochrome P450 reductase gene in the cotton bollworm, *Helicoverpa armigera*. *Pest Manag Sci.* 2014;70: 130–139. doi:10.1002/ps.3538
122. Wang H, Luo J, Chen Z, Cao WT, Xu HF, Gou DM, et al. MicroRNA-24 can control triacylglycerol synthesis in goat mammary epithelial cells by targeting the fatty acid synthase gene. *J Dairy Sci.* 2015;98: 9001–9014. doi:10.3168/jds.2015-9418
123. Bhatia H, Verma G, Datta M. miR-107 orchestrates ER stress induction and lipid accumulation by post-transcriptional regulation of fatty acid synthase in hepatocytes. *Biochimica Et Biophysica Acta Bba - Gene Regul Mech.* 2014;1839: 334–343. doi:10.1016/j.bbagr.2014.02.009
124. Benatti RO, Melo AM, Borges FO, Ignacio-Souza LM, Simino LAP, Milanski M, et al. Maternal high-fat diet consumption modulates hepatic lipid metabolism and microRNA-122 (miR-122) and microRNA-370 (miR-370) expression in offspring. *Brit J Nutr.* 2014;111: 2112–2122. doi:10.1017/s0007114514000579
125. Wahdan-Alaswad RS, Cochrane DR, Spoelstra NS, Howe EN, Edgerton SM, Anderson SM, et al. Metformin-Induced Killing of Triple-Negative Breast Cancer Cells Is Mediated by Reduction in Fatty Acid Synthase via miRNA-193b. *Hormones Cancer.* 2014;5: 374–389. doi:10.1007/s12672-014-0188-8
126. Wang X-C, Zhan X-R, Li X-Y, Yu J-J, Liu X-M. MicroRNA-185 regulates expression of lipid metabolism genes and improves insulin sensitivity in mice with non-alcoholic fatty liver disease. *World J Gastroentero.* 2014;20: 17914–17923. doi:10.3748/wjg.v20.i47.17914
127. LONG XH, MAO JH, PENG AF, ZHOU Y, HUANG SH, LIU ZL. Tumor suppressive microRNA-424 inhibits osteosarcoma cell migration and invasion via targeting fatty acid synthase. *Exp Ther Med.* 2013;5: 1048–1052. doi:10.3892/etm.2013.959
128. MAO JH, ZHOU RP, PENG AF, LIU ZL, HUANG SH, LONG XH, et al. microRNA-195 suppresses osteosarcoma cell invasion and migration in vitro by targeting FASN. *Oncol Lett.* 2012;4: 1125–1129. doi:10.3892/ol.2012.863
129. Iliopoulos D, Drosatos K, Hiyama Y, Goldberg IJ, Zannis VI. MicroRNA-370 controls the expression of MicroRNA-122 and Cpt1 α and affects lipid metabolism[S]. *J Lipid Res.* 2010;51: 1513–1523. doi:10.1194/jlr.m004812

130. Naggar YA, Wiseman S, Jianxian S, Cutler GC, Aboul-Soud M, Naiem E, et al. Effects of environmentally-relevant mixtures of four common organophosphorus insecticides on the honey bee (*Apis mellifera* L.). *J Insect Physiol.* 2015;82: 85–91. doi:10.1016/j.jinsphys.2015.09.004
131. Feyereisen R. Insect CYP genes and P450 enzymes. *Insect molecular biology and biochemistry.* 2013; 236–316.
132. Murataliev MB, Guzov VM, Walker FA, Feyereisen R. P450 reductase and cytochrome b 5 interactions with cytochrome P450: Effects on house fly CYP6A1 catalysis. *Insect Biochem Molec.* 2008;38: 1008–1015. doi:10.1016/j.ibmb.2008.08.007
133. Qiu Y, Tittiger C, Wicker-Thomas C, Goff GL, Young S, Wajnberg E, et al. An insect-specific P450 oxidative decarbonylase for cuticular hydrocarbon biosynthesis. *Proc National Acad Sci.* 2012;109: 14858–14863. doi:10.1073/pnas.1208650109
134. Jin X, Wu X, Zhou L, He T, Yin Q, Liu S. 20-Hydroxyecdysone-responsive microRNAs of insects. *Rna Biol.* 2020;17: 1454–1471. doi:10.1080/15476286.2020.1775395
135. Freitas FCP, Pires CV, Claudianos C, Cristino AS, Simões ZLP. MicroRNA-34 directly targets pair-rule genes and cytoskeleton component in the honey bee. *Sci Rep-uk.* 2017;7: 40884. doi:10.1038/srep40884
136. Zhang B, Li H, Li D, Sun H, Li M, Hu H. Long noncoding RNA Mirt2 upregulates USP10 expression to suppress hepatic steatosis by sponging miR-34a-5p. *Gene.* 2019;700: 139–148. doi:10.1016/j.gene.2019.02.096
137. Lyons PJ, Crapoulet N, Storey KB, Morin PJ. Identification and profiling of miRNAs in the freeze-avoiding gall moth *Epiblema scudderiana* via next-generation sequencing. *Mol Cell Biochem.* 2015;410: 155–163. doi:10.1007/s11010-015-2547-3
138. Chandra S, Pandey A, Chowdhuri DK. miRNA profiling provides insights on adverse effects of Cr(VI) in the midgut tissues of *Drosophila melanogaster*. *J Hazard Mater.* 2015;283: 558–567. doi:10.1016/j.jhazmat.2014.09.054
139. Courteau LA, Storey KB, Morin PJr. Differential expression of microRNA species in a freeze tolerant insect, *Eurosta solidaginis*. *Cryobiology.* 2012;65: 210–214. doi:10.1016/j.cryobiol.2012.06.005
140. Kugler J-M, Verma P, Chen Y-W, Weng R, Cohen SM. miR-989 Is Required for Border Cell Migration in the *Drosophila* Ovary. *Plos One.* 2013;8: e67075. doi:10.1371/journal.pone.0067075
141. Peng W, Tariq K, Xie J, Zhang H. Identification and Characterization of Sex-Biased MicroRNAs in *Bactrocera dorsalis* (Hendel). *Plos One.* 2016;11: e0159591. doi:10.1371/journal.pone.0159591

142. Liu W, Huang H, Xing C, Li C, Tan F, Liang S. Identification and characterization of the expression profile of microRNAs in *Anopheles anthropophagus*. *Parasite Vector*. 2014;7: 159–159. doi:10.1186/1756-3305-7-159
143. Marco A. Sex-biased expression of microRNAs in *Drosophila melanogaster*. *Open Biol*. 2014;4: 140024. doi:10.1098/rsob.140024
144. Begna D, Fang Y, Feng M, Li J. Mitochondrial Proteins Differential Expression during Honeybee (*Apis mellifera* L.) Queen and Worker Larvae Caste Determination. *J Proteome Res*. 2011;10: 4263–4280. doi:10.1021/pr200473a
145. Hsin J-P, Lu Y, Loeb GB, Leslie CS, Rudensky AY. The effect of cellular context on miR-155-mediated gene regulation in four major immune cell types. *Nat Immunol*. 2018;19: 1137–1145. doi:10.1038/s41590-018-0208-x
146. Stark A, Bushati N, Jan CH, Kheradpour P, Hodges E, Brennecke J, et al. A single Hox locus in *Drosophila* produces functional microRNAs from opposite DNA strands. *Gene Dev*. 2008;22: 8–13. doi:10.1101/gad.1613108
147. Tyler DM, Okamura K, Chung W-J, Hagen JW, Berezikov E, Hannon GJ, et al. Functionally distinct regulatory RNAs generated by bidirectional transcription and processing of microRNA loci. *Gene Dev*. 2008;22: 26–36. doi:10.1101/gad.1615208
148. Wolfson RL, Chantranupong L, Wyant GA, Gu X, Orozco JM, Shen K, et al. KICSTOR recruits GATOR1 to the lysosome and is necessary for nutrients to regulate mTORC1. *Nature*. 2017;543: 438–442. doi:10.1038/nature21423
149. Niño EL, Tarpay DR, Grozinger CM. Differential effects of insemination volume and substance on reproductive changes in honey bee queens (*Apis mellifera* L.). *Insect Mol Biol*. 2013;22: 233–244. doi:10.1111/imb.12016
150. Laidlaw HH, Page RE. Queen rearing and bee breeding. Wicwas Press; 1998.
151. Dade HA. Anatomy and dissection of the honeybee. IBRA; 1995.
152. Hess G. Ueber den Einfluss der Weisellosigkeit und des Fruchtbarkeitsvitamins E auf die Ovarien der Bienenarbeiterin: ein Beitrag zur Frage der Regulationen im Bienenstaat. 1943.
153. Buschmann D, Haberberger A, Kirchner B, Spornraft M, Riedmaier I, Schelling G, et al. Toward reliable biomarker signatures in the age of liquid biopsies - how to standardize the small RNA-Seq workflow. *Nucleic Acids Res*. 2016;44: 5995–6018. doi:10.1093/nar/gkw545
154. Baran-Gale J, Kurtz CL, Erdos MR, Sison C, Young A, Fannin EE, et al. Addressing Bias in Small RNA Library Preparation for Sequencing: A New Protocol Recovers MicroRNAs that Evade Capture by Current Methods. *Frontiers Genetics*. 2015;6: 352. doi:10.3389/fgene.2015.00352

155. Andrews S. FastQC: a quality control tool for high throughput sequence data. 2012. Available: www.bioinformatics.babraham.ac.uk/projects/fastqc/
156. Martin M. Cutadapt removes adapter sequences from high-throughput sequencing reads. *Embnet J.* 2011;17: 10–12. doi:10.14806/ej.17.1.200
157. Gordon A, Hannon G. Fastx-toolkit. 2010. Available: http://hannonlab.cshl.edu/fastx_toolkit
158. Friedländer MR, Mackowiak SD, Li N, Chen W, Rajewsky N. miRDeep2 accurately identifies known and hundreds of novel microRNA genes in seven animal clades. *Nucleic Acids Res.* 2012;40: 37–52. doi:10.1093/nar/gkr688
159. Mackowiak SD. Identification of Novel and Known miRNAs in Deep - Sequencing Data with miRDeep2. *Curr Protoc Bioinform.* 2011;36: 12.10.1-12.10.15. doi:10.1002/0471250953.bi1210s36
160. Wallberg A, Bunikis I, Pettersson OV, Mosbech M-B, Childers AK, Evans JD, et al. A hybrid de novo genome assembly of the honeybee, *Apis mellifera*, with chromosome-length scaffolds. *Bmc Genomics.* 2019;20: 275. doi:10.1186/s12864-019-5642-0
161. Griffiths-Jones S, Saini HK, Dongen S van, Enright AJ. miRBase: tools for microRNA genomics. *Nucleic Acids Res.* 2008;36: D154–D158. doi:10.1093/nar/gkm952
162. Law CW, Chen Y, Shi W, Smyth GK. voom: precision weights unlock linear model analysis tools for RNA-seq read counts. *Genome Biol.* 2014;15: R29–R29. doi:10.1186/gb-2014-15-2-r29
163. Langfelder P, Zhang B, Horvath S. Defining clusters from a hierarchical cluster tree: the Dynamic Tree Cut package for R. *Bioinformatics.* 2007;24: 719–720. doi:10.1093/bioinformatics/btm563
164. Langfelder P, Horvath S. WGCNA: an R package for weighted correlation network analysis. *Bmc Bioinformatics.* 2008;9: 559–559. doi:10.1186/1471-2105-9-559
165. Miranda KC, Huynh T, Tay Y, Ang Y-S, Tam W-L, Thomson AM, et al. A Pattern-Based Method for the Identification of MicroRNA Binding Sites and Their Corresponding Heteroduplexes. *Cell.* 2006;126: 1203–1217. doi:10.1016/j.cell.2006.07.031
166. REHMSMEIER M, STEFFEN P, HÖCHSMANN M, GIEGERICH R. Fast and effective prediction of microRNA/target duplexes. *Rna.* 2004;10: 1507–1517. doi:10.1261/rna.5248604
167. Enright AJ, John B, Gaul U, Tuschl T, Sander C, Marks DS. MicroRNA targets in *Drosophila*. *Genome Biol.* 2003;5: R1–R1. doi:10.1186/gb-2003-5-1-r1

168. Wessels H-H, Lebedeva S, Hirsekorn A, Wurmus R, Akalin A, Mukherjee N, et al. Global identification of functional microRNA-mRNA interactions in *Drosophila*. *Nat Commun*. 2019;10: 1626. doi:10.1038/s41467-019-09586-z
169. Zhang K, Zhang X, Cai Z, Zhou J, Cao R, Zhao Y, et al. A Novel Class of MicroRNA Recognition Elements That Function Only in Open Reading Frames. *Nat Struct Mol Biol*. 2018;25: 1019–1027. doi:10.1038/s41594-018-0136-3
170. Liu G, Zhang R, Xu J, Wu C-I, Lu X. Functional Conservation of Both CDS- and 3' - UTR-Located MicroRNA Binding Sites between Species. *Mol Biol Evol*. 2014;32: 623–628. doi:10.1093/molbev/msu323
171. Brümmer A, Hausser J. MicroRNA binding sites in the coding region of mRNAs: Extending the repertoire of post - transcriptional gene regulation. *Bioessays*. 2014;36: 617–626. doi:10.1002/bies.201300104
172. Helwak A, Kudla G, Dudnakova T, Tollervey D. Mapping the Human miRNA Interactome by CLASH Reveals Frequent Noncanonical Binding. *Cell*. 2013;153: 654–665. doi:10.1016/j.cell.2013.03.043
173. Reczko M, Maragkakis M, Alexiou P, Grosse I, Hatzigeorgiou AG. Functional microRNA targets in protein coding sequences. *Bioinformatics*. 2012;28: 771–776. doi:10.1093/bioinformatics/bts043
174. Zhou X, Duan X, Qian J, Li F. Abundant conserved microRNA target sites in the 5' - untranslated region and coding sequence. *Genetica*. 2009;137: 159–164. doi:10.1007/s10709-009-9378-7
175. Agarwal V, Bell GW, Nam J-W, Bartel DP. Predicting effective microRNA target sites in mammalian mRNAs. *Elife*. 2015;4: e05005. doi:10.7554/elife.05005
176. Kriventseva EV, Kuznetsov D, Tegenfeldt F, Manni M, Dias R, Simão FA, et al. OrthoDB v10: sampling the diversity of animal, plant, fungal, protist, bacterial and viral genomes for evolutionary and functional annotations of orthologs. *Nucleic Acids Res*. 2018;47: D807–D811. doi:10.1093/nar/gky1053
177. Plaisier SB, Taschereau R, Wong JA, Graeber TG. Rank–rank hypergeometric overlap: identification of statistically significant overlap between gene-expression signatures. *Nucleic Acids Res*. 2010;38: e169–e169. doi:10.1093/nar/gkq636
178. Bailey TL, Boden M, Buske FA, Frith M, Grant CE, Clementi L, et al. MEME Suite: tools for motif discovery and searching. *Nucleic Acids Res*. 2009;37: W202–W208. doi:10.1093/nar/gkp335
179. Geiduschek EP, Tocchini-Valentini GP. Transcription by RNA Polymerase III. *Annu Rev Biochem*. 2020;57: 873–914. doi:10.1146/annurev.bi.57.070188.004301

180. Ngoc LV, Kassavetis GA, Kadonaga JT. The RNA Polymerase II Core Promoter in *Drosophila*. *Genetics*. 2019;212: 13–24. doi:10.1534/genetics.119.302021
181. Knudsen S. Promoter2.0: for the recognition of PolIII promoter sequences. *Bioinformatics*. 1999;15: 356–361. doi:10.1093/bioinformatics/15.5.356
182. Shannon P, Markiel A, Ozier O, Baliga NS, Wang JT, Ramage D, et al. Cytoscape: A Software Environment for Integrated Models of Biomolecular Interaction Networks. *Genome Res*. 2003;13: 2498–2504. doi:10.1101/gr.1239303
183. Bindea G, Mlecnik B, Hackl H, Charoentong P, Tosolini M, Kirilovsky A, et al. ClueGO: a Cytoscape plug-in to decipher functionally grouped gene ontology and pathway annotation networks. *Bioinformatics*. 2009;25: 1091–1093. doi:10.1093/bioinformatics/btp101
184. Cristino AS, Barchuk AR, Freitas FCP, Narayanan RK, Biergans SD, Zhao Z, et al. Neuroligin-associated microRNA-932 targets actin and regulates memory in the honeybee. *Nat Commun*. 2014;5: 5529. doi:10.1038/ncomms6529
185. Mi H, Ebert D, Muruganujan A, Mills C, Albou L-P, Mushayamaha T, et al. PANTHER version 16: a revised family classification, tree-based classification tool, enhancer regions and extensive API. *Nucleic Acids Res*. 2020;49: gkaa1106-. doi:10.1093/nar/gkaa1106
186. Hammer TJ, Hata C, Nieh JC. Thermal learning in the honeybee, *Apis mellifera*. *J Exp Biol*. 2009;212: 3928–3934. doi:10.1242/jeb.034140
187. Bitterman ME, Menzel R, Fietz A, Schäfer S. Classical conditioning of proboscis extension in honeybees (*Apis mellifera*). *J Comp Psychol*. 1983;97: 107–119. doi:10.1037/0735-7036.97.2.107